2002

The impact of fixturing error on feature tolerance allocation

Supapan Sangnui
Iowa State University

INFORMATION TO USERS

This manuscript has been reproduced from the microfilm master. UMI films the text directly from the original or copy submitted. Thus, some thesis and dissertation copies are in typewriter face, while others may be from any type of computer printer.

The quality of this reproduction is dependent upon the quality of the copy submitted. Broken or indistinct print, colored or poor quality illustrations and photographs, print bleedthrough, substandard margins, and improper alignment can adversely affect reproduction.

In the unlikely event that the author did not send UMI a complete manuscript and there are missing pages, these will be noted. Also, if unauthorized copyright material had to be removed, a note will indicate the deletion.

Oversize materials (e.g., maps, drawings, charts) are reproduced by sectioning the original, beginning at the upper left-hand corner and continuing from left to right in equal sections with small overlaps.

ProQuest Information and Learning
300 North Zeeb Road, Ann Arbor, MI 48106-1346 USA
800-521-0600

The impact of fixturing error on feature tolerance allocation

by

Supapan Sangnui

A dissertation submitted to the graduate faculty

in partial fulfillment of the requirements for the degree of

DOCTOR OF PHILOSOPHY

Major: Industrial Engineering

Program of Study Committee:
Frank Peters, Major Professor
John Jackman
Palaniappa Molian
Timothy VanVoorhis
Stephen Vardeman

Iowa State University

Ames, Iowa

2002

UMI Number: 3074117

UMI Microform 3074117

ProQuest Information and Learning Company
300 North Zeeb Road
P.O. Box 1346
Ann Arbor, MI 48106-1346

Graduate College
Iowa State University

This is to certify that the doctoral dissertation of

Supapan Sangnui

has met the dissertation requirements of Iowa State University

Signature was redacted for privacy.

Major Professor

Signature was redacted for privacy.

For the Major Program

TABLE OF CONTENTS

LIST OF FIGURES

CHAPTER 1.

CHAPTER 2.

CHAPTER 3.

APPENDIX A.

APPENDIX B.

LIST OF TABLES

CHAPTER 2.

CHAPTER 3.

ABSTRACT

Fixtures are used to locate, hold and support workpieces during the operation. An accuracy of the workpiece is decided by a relative location and orientation of the workpiece coordinate system with respect to that of the fixture. The impact of surface variability at contact points on the variability of workpiece location and orientation will be analyzed. Methods of estimating moments will be implemented to evaluate the distribution of the workpiece variability. When surface errors exist and the workpiece is fixtured for machining, inconsistency in feature location and orientation is expected. Hence, in order to derive efficient tolerance allocation for the feature, the fixturing error must be taken into account. A circular tolerance region based on a bivariate normal distribution will be used to obtain tolerance zones of a desired probability of rejection. By establishing tolerance efficiently, we can reduce a number of rejected parts, leading to some reduction in production cost and time.

CHAPTER 1. GENERAL INTRODUCTION

INTRODUCTION

In a competitive market-driven world, manufacturing companies are in search of technologies that can improve product quality, which will in turn give them the competitiveness in the market and customer satisfaction. Establishing an efficient process plan is one way to attain such goals. However, to do so requires collaboration among many departments especially from the design and manufacturing divisions. For example, when a company agrees to take on a new product, it would need a designer to develop a physical model that meets the product's functional requirements. At this stage, the designer may team up with manufacturing engineers to discuss ways of producing the part. It is clear that process planning is the vital link between the product design and manufacturing. An important aspect of the process plan is the fixture design. Fixturing analysis is a critical part of process planning as it contributes up to 10-20% on average of the total production cost [1]. As a result, the interaction between the fixture and the workpiece should be considered from the design stage so that the analysis of fixture can be conducted as the design progresses.

Fixtures are used to locate, hold and support workpieces during manufacturing operations. The relative position and orientation of a workpiece coordinate system with respect to a fixture coordinate system are key to determine geometrical and dimensional accuracy of final products. In machining, there are many factors threatening the accuracy of the workpiece position while it is fixtured. Such factors include machine vibration, fixturing error, workpiece or fixture deformation, cutting force, and surface error at contact points. Research has been widely carried out in this area; however, only a few researchers have

taken into account the effect of surface errors upon the efficiency of workpiece positioning. This thesis proposes a new approach of fixture analysis by integrating the impact of workpiece surface error into feature tolerancing. Our focus is on the deviation prior to machining which is caused by the surface variability at the contact points between workpiece and a fixture. Typically, quality of the surface error is dependent on the preceding process and the process parameters, as shown in Figure 1.

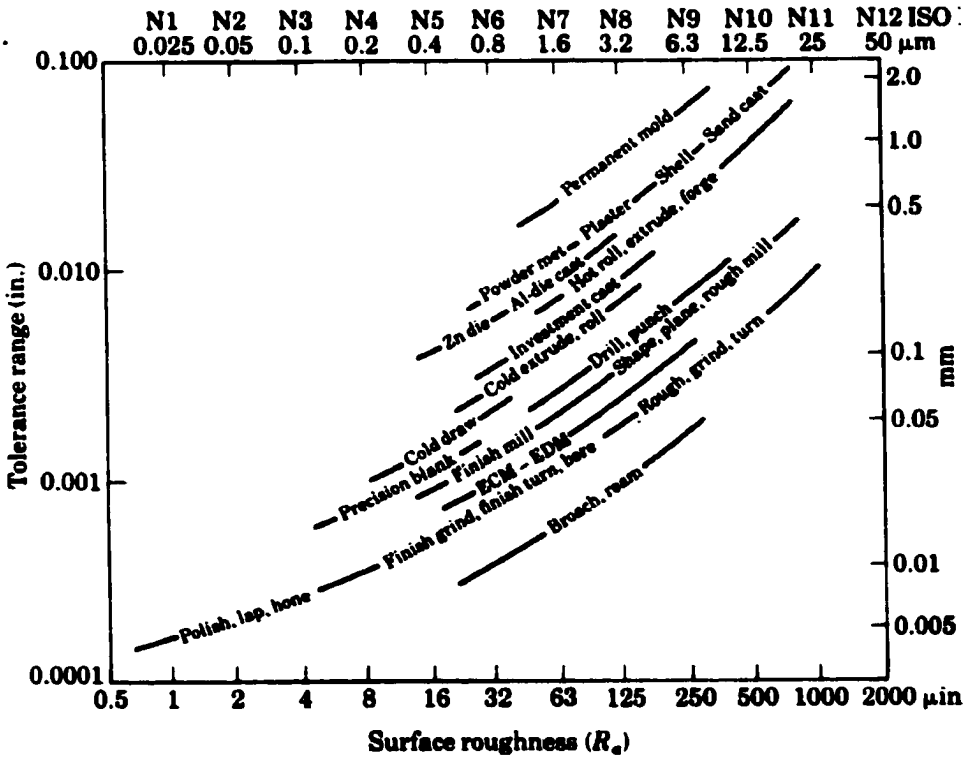

Figure 1. Tolerances and surface roughness obtained in various manufacturing processes. These tolerances apply to 25 mm workpiece dimension. Source: S. Kalpakjian [2].

Surface variability, in most occasions, is inevitable. With the existence of the variability, the workpiece is prone to displace from its nominal location and orientation. If

the preceding process does not provide a surface with acceptable surface errors, rough machining of the contact areas is advised. To minimize the effect of surface errors, datum targets are established to improve the repeatability of workpiece location and orientation. Datum targets are expected contact points (or areas), and are typically selected such that the surface irregularities are minimal. They are more functional than the use of entire surfaces for the establishment of datums [3]. However, the use of datum targets will not completely eliminate the effect of surface errors on workpiece locating, therefore, it will not guarantee successful mapping of the workpiece coordinate system with that of the fixture. It is thus suggested to understand the impact of the variability on a resultant workpiece quality. The allowable surface error or variability, may not severely affect the production process as a whole. However, it could introduce significant errors during processing.

It is therefore favorable if the process planner and the fixture designer have a better perception on the behavior, with regard to the surface error at contact points, of the workpiece while it is held in a fixture. Fixture handbooks exist to give qualitative advice to these designers and planners to design a functional fixture [4]. The method developed in this work will provide the planners and designers with quantitative information about the effect of the fixture design decision or workpiece errors. Based on this information, the fixture could be redesigned in a way that it will repeatabily position the workpiece closest to its theoretical location and orientation. Contact points could be relocated to areas of the workpiece offering the most accurate workpiece positioning. In addition, understanding how the variable behavior of the workpiece contributes to feature tolerancing is as important. This information could be used to specify the tolerances needed for the preceding process, and to define reasonable tolerances of descendant features. Features will never be efficiently

toleranced unless all factors listed previously are accounted for. The objective of this thesis is to analyze the impact of workpiece surface errors on feature tolerancing. The 3-2-1 fixturing method, which is composed of three mutually perpendicular references, is used. These ideal planes are constructed from six contact points between the workpiece and locators; for example, three for the primary datum plane, two for the secondary datum plane, and one for the tertiary datum plane. The workpiece is to make contact with all the locators in the primary datum plane first, followed by the locators in the secondary and then the tertiary datum plane.

Tolerances are thus established to permit parts with acceptable errors in dimension and geometry to be accepted, resulting in reduction in production cost and time. Many tolerancing methods have been proposed to control variability in manufacturing and some of them are industry standards. Statistical tolerancing is the one, which is widely used because of its advantages over conventional methods as follows [5];

1. Conventional methods treat the tolerances as limits on the parameters of a parametric model. However, as geometric tolerancing represented by tolerance zones instead of limits is more widely accepted, conventional methods become more awkward.

2. In assembly, tolerances built up from either worst-case methods or root-sum-squares method are not accurate. Worst-case methods give results that are overly pessimistic, while the root-sum-squares method gives results that are too optimistic.

As a result, probabilistic models better represent the variation in manufacturing processes, and bridge the gap between this variation and the geometric tolerancing. The distribution which best describes the variability in manufacturing is controversial. Despite some opposition [6, 7], many researchers [8-10] use a normal or Gaussian distribution to represent such variability. If the event of interest randomly occurs and the sample size is

large enough, a normal distribution seems to be an excellent candidate. Even though the sample is not random, we can still theoretically assume a normal distribution with a large sample size by following the central limit theorem. Likewise, a normal distribution is adopted in the first part of this thesis to denote the variable nature of surface errors. Such errors are known to introduce variability in workpiece positioning, consequently in feature dimension and geometry, for which a normal distribution is proven to be a reasonable estimate.

There are several publications found relevant to fixturing error in manufacturing processes. Only a few researchers investigated the displacement of a workpiece's location and orientation in a fixture caused by surface errors at contact points, which are discussed in the next section.

LITERATURE REVIEW

Salisbury and Peters [11] have given closer attention at the impact of surface errors on the deviation of workpiece location and orientation. They developed a model to predict the deviation of a prismatic workpiece located by 3-2-1 fixturing method. The workpiece came into contact with the fixture through a virtual step-wise process. The workpiece was then modeled as making contact with one locator at a time and the process continued until the workpiece touched all six locators. This model was developed under a worst-case scenario. Given the surface errors at contact points, the location of a target point and orientation of the workpiece can be obtained. However, the result indicated that the largest deviation does not necessarily come from the largest errors at the contact points.

Later, the mathematical model of this purpose for a cylindrical workpiece was developed by Sangnui and Peters [12]. An algorithm was created in order to study a relationship between the workpiece and fixture coordinate systems. The fixture was composed of five spherical-tipped locators, used to hold and restrain workpiece movements. The workpiece and fixture coordinate systems were defined separately. The constraints were established to assure the contact between the workpiece and these locators. To find the position and orientation of the cylinder that satisfy the constraints, the cylinder was repeatedly virtually rotate around its origin before being translated by a certain distance. The mapping between both coordinate systems can be derived through a transformation of the cylinder. Experiments were conducted to determine validity of the model and repeatability of the equipment.

The previous work assumed a worst-case scenario and disregarded the probabilistic concept. To fill this void, the probabilistic nature of the surface errors will be considered in the first part of this thesis. A prismatic workpiece is located by 3-2-1 fixturing method and its location and orientation are also analyzed using step-wise approach. The objective of this work is to acquire the distribution of a target point location, as well as the distribution of the workpiece orientation. Methods of estimating moments, linearization by using Taylor series [5, 13] and Monte Carlo simulation, will be performed and results from both methods will be compared. Because of an inconsistency in location and orientation of the workpiece coordinate system with respect to the fixture coordinate system, variability in feature position and orientation is expected. In the second part, the effect of the workpiece displacement on tolerance allocation of features of subsequent machining will be analyzed.

DISSERTATION ORGANIZATION

This dissertation contains two papers to be submitted to journals, which appear in separate chapters. In Chapter 2, the first paper; *Prediction of Fixtured Workpiece Location when there are Variable Surface Errors at the Fixturing Points*, discusses the effect of distributions of surface errors at contact points on workpiece location and orientation. Applications of the model developed in the first paper on tolerance allocation of machined features are illustrated in Chapter 3. The chapter is dedicated to the second paper; *Determination of Appropriate Tolerances of Machine Features when there are Surface Errors at the Fixturing Points*. General introduction and conclusion are in Chapter 1 and 4, respectively.

REFERENCES

1.Fuh, J.Y.H., C.-H. Chang, and M.A. Melkanoff, *An integrated fixture planning and analysis system for machining processes.* Robotics and Computer-integrated Manufacturing, 1993. 10: p. 339-353.

2.Kalpakjian, S., *Manufacturing Processes for Enigneering Materials*. 2nd ed. 1991: Addison-Wesley Publishing Company, Inc.

3.Meadows, J.D., *Geometric dimensioning and tolerancing: applications and techniques for use in design, manufacturing, and inspection*. 1995, New York, NY: Marcel Dekker, Inc.

4.*Handbook of Jig and Fixture Design*. 2nd ed, ed. W.E. Boyes. 1989, Dearborn, MI: Society of Manufacturing Engineers.

5.Nigam, S.D. and J.U. Turner, *Review of statistical approaches to tolerance analysis.* Computer Aided Design, 1995. 27(1): p. 6-15.

6.Lin, S.-S., H.-P. Wang, and C. Zhang, *Statistical tolerance analysis based on beta distributions.* Journal of Manufacturing Systems, 1997. 16: p. 150-8.

7.He, J.R., *Estimating the distributions of manufactured dimensions with the beta probability density function.* International Journal of Machine Tools & Manufacture, 1991. 31(3): p. 38.-396.

8.Evans, D.H., *An application of numerical integration techniques to statistical tolerancing.* Technometrics, 1967. 9(3): p. 441-456.

9.Evans, D.H., *An application of numerical integration techniques to statistical tolerancing, III General distributions.* Technometrics, 1972. 14(1): p. 23-35.

10.Nassef, A.O. and H.A. ElMaraghy, *Statistical analysis and optimal allocation of geometric tolerances.* Proceedings of the 1995 Database Symposium, ASME Database Symposium, 1995: p. 817-824.

11.Salisbury, E.J. and F.E. Peters, *The impact of surface errors on fixtured workpiece location and orientation.* NAMRC Transactions, 1998. 26: p. 323-328.

12.Sangnui, S. and F.E. Peters, *The impact of surface errors on the location and orientation of a cylindrical workpiece in a fixture.* Journal of Manufacturing Science and Engineering, 2001. 123.

13.Evans, D.H., *Statistical tolerancing: the state of the art, pt. 2 methods for estimating moments.* Journal of Quality Technology, 1975.

CHAPTER 2. PREDICTION OF FIXTURED WORKPIECE LOCATION WHEN THERE ARE VARIABLE SURFACE ERRORS AT THE FIXTURING POINTS

A paper to be submitted to the Journal of Manufacturing Science and Engineering

Supapan Sangnui and Frank E. Peters

ABSTRACT

In this paper, it is assumed that surface variability is normally distributed. Similar to the previous work by Salisbury and Peters [1], a prismatic workpiece is located by 3-2-1 fixturing method and its location and orientation are also analyzed using step-wise approach. However, the steps are modified such that they become more systematic and computationally easier to handle. The objective of this work is to acquire a distribution of a target point location, as well as that of the workpiece orientation. This is not straightforward, since the response function is non-linear and derived through a set of complicated equations. Two methods of estimating moments, linearization by using Taylor series and Monte Carlo simulation, will be performed and the results from both methods will be compared.

LIST OF SYMBOLS

d_i	surface error at i^{th} locator
D_s, D_t	distance that the workpiece translates to make contact with the secondary and tertiary planes, respectively
l_s, l_t	distance from the origin to the workpiece secondary and tertiary planes, respectively
$\bar{N}_p$, $\bar{N}_s$, $\bar{N}_t$	initial normal vector of the primary, secondary and tertiary planes, respectively
$\bar{N}'_p$, $\bar{N}'_s$, $\bar{N}'_t$	normal vector of the primary, secondary, and tertiary planes, respectively, after transformation due to variability in the primary plane
$\bar{N}''_s$, $\bar{N}''_t$	normal vector of the secondary and tertiary planes, respectively, after transformation due to variability in the secondary plane
$\bar{o}$	vector to the nominal target point on the workpiece
$\bar{o}_{pt}$, $\bar{o}_{pr}$	vector to the target point after translation and rotation in the primary plane, respectively
$\bar{o}_{st}$, $\bar{o}_{sr}$	vector to the target point after translation and rotation in the secondary plane, respectively
$\bar{o}_t$	vector to the target point after translation in the tertiary plane
P_i	point that the nominal workpiece makes contact with i^{th} locator
P_{id}	point that the workpiece makes contact with i^{th} locator (including surface error), with respect to the fixture coordinate system
$P_{i\mu}$	expected points that the workpiece makes contact with i^{th} locator (including mean of surface error), with respect to the fixture coordinate system
T_p, T_s	transformation matrix used to rotate the workpiece to make contact with the primary and secondary plane respectively
u_p, u_s	axis that the workpiece rotates about to make contact with the primary and secondary plane respectively
θ_p, θ_s	angle that the workpiece rotates to make contact with the primary and secondary plane respectively
μ_i	mean of surface error at i^{th} locator
σ_i^2	variance of surface error at i^{th} locator
M_N	set of $\mu_1,..\mu_n$
δ_N	set of $d_1,..d_n$

INTRODUCTION

Fixtures are used to properly locate and orient a workpiece with respect to a machine tool. Since an accuracy of the workpiece is mainly determined through the relative location and orientation of the workpiece to the tool, fixtures are thus a critical part of a manufacturing system. There are several variables, which will cause the workpiece to deviate from the desired position, and the fixture is responsible for minimizing or controlling their effect. Such variables include cutting and clamping force, workpiece deflection, fixture set-up error, and workpiece surface error at the locating points. A typical 3-2-1 fixturing method is composed of the primary, secondary and tertiary datum planes. Theoretically, the contact is to take place at the nominal contact locations. However, no matter what manufacturing process is used to create the initial workpiece, surface irregularities at the contact locations are inevitable, resulting in some discrepancy between the nominal and actual contact points. Given a distribution of the surface errors at the contact locations, statistics allows us to derive variability of the final position and orientation of the workpiece.

This paper will develop a method to calculate the influence of variable surface errors at the locating points on the accuracy of the workpiece. By utilizing the information obtained from this method, a designer can select appropriate tolerances required for the initial workpiece and can predict the variation of subsequent processes. Ultimately, the fixture can be designed to reduce the effect of inevitably erratic workpiece locating.

LITERATURE REVIEW

Researchers working in the fixturing area have developed algorithms that provide complete constraint of the workpiece [2-8], determined sufficient support and performance of the fixture [9-13] and accessibility[14]. Less focus has been placed on determining the initial displacement of the workpiece in the fixture.

Rong and Bai [13] analyzed a dependent relationship of operational dimensions to estimate machining errors in terms of linear and angular dimensions of the workpiece. Based on an analysis of machining processes, machining errors were divided into deterministic and random components. The deterministic machining errors are caused by locating errors of the fixture, position errors of the fixture, locating component and datum variation of the workpiece. The authors determined the effect of random errors caused by clamping deformation, cutting forces and thermal deformation.

Cai et al. [3] proposed a method to conduct robust fixture design to minimize the workpiece positional errors as a result of workpiece surface and fixture set-up errors. It was shown that when the rank of the Jacobian matrix of the constraint equations equaled the degrees of freedom of the workpiece, the deterministic locating condition would be achieved.

Choudhuri and De Meter [15] developed a method for modeling and analyzing the impact of a locator tolerance scheme on the potential datum related, geometric errors of linear, machined features. This study was limited to profile and dimensional tolerances applied to spherical tip locators in contact with planar workpiece. The results reveal the linear relationship between locator tolerance size and resultant datum related geometric error. The study suggested the use of larger locator radii in order to minimize the impact of the contact region deformation on the workpiece displacement during clamping. They also

found that datum related geometric error due to locator variability was sensitive to the source of locator variability but not to the locator radius.

Salisbury and Peters [1] presented a model to predict a deviation of a prismatic workpiece located by 3-2-1 fixturing method. The workpiece came into contact with the fixture through a virtual step-wise process. The workpiece was then modeled as if it makes contact with one locator at a time and the process continued until the workpiece touched all six locators. Note that, this model was developed under a static case scenario. Given a constant value of surface errors at the contact points, the location of a target point on the workpiece and the orientation of the workpiece could be obtained. The results indicated that the largest deviation did not necessarily came from the largest errors at the contact points.

Later, the mathematical model of the same purpose for a cylindrical workpiece was established by Sangnui and Peters [16]. An algorithm was created to study a relationship between a workpiece and fixture coordinate systems, which was influenced by surface variability at contact points. The fixture was composed of five spherical-tipped locators, used to hold and restrain workpiece movements. The constraints were established to assure the contact between the workpiece and these locators. The workpiece and fixture coordinate systems were defined separately. The cylinder was assumed to rotate around its origin and then translated a certain distance to contact all locators. The mapping between both coordinate systems could be derived through the transformation of the cylinder. Experiments were conducted to determine the validity of the model, and the repeatability of the equipment.

METHODOLOGY

The previous work assumed a worst-case scenario and disregarded the probabilistic concept. In the current work, the probabilistic nature of the surface errors will be considered. The purpose of the algorithm presented in this section is to acquire the position and orientation of a workpiece under the influence of surface errors after the workpiece has made contact with each datum plane. A method to determine the variable location and orientation of a prismatic workpiece, which is held by the 3-2-1 fixturing method is developed. To assure repeatability of the workpiece location and orientation, the workpiece is required to initially make contact with 3 datum targets in the primary plane (points 1-3), followed by 2 datum targets in the secondary plane (points 4-5) and finally, the last datum target in the tertiary plane (point 6), see Figure 1.

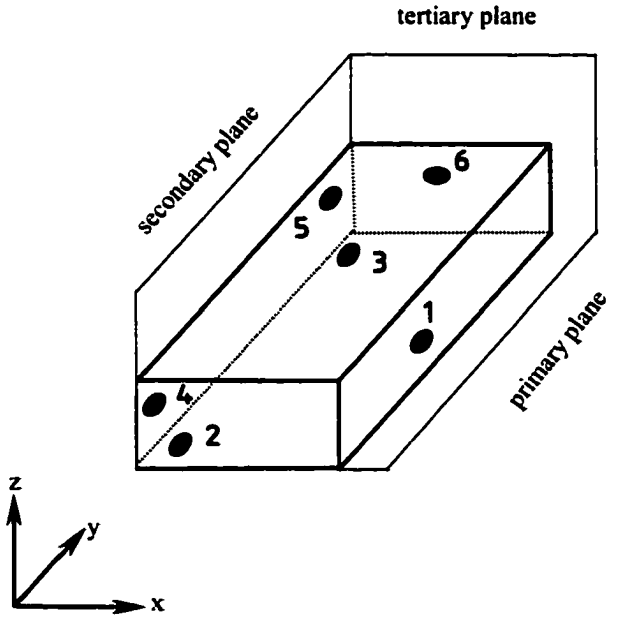

Figure 1. Locating planes and datum targets in 3-2-1 fixture.

ASSUMPTIONS

Several assumptions regarding the fixture and the surface error model were used and are shown below.

1. A workpiece is considered a rigid body. Deformation of the workpiece during transformation is not allowed.

2. Errors at contact points are assumed to be normally distributed with mean μ and variance σ^2, or $N(\mu, \sigma^2)$.

3. The errors are measured perpendicularly to the datum planes. The determination of the surface error sign is shown in Figure 2.

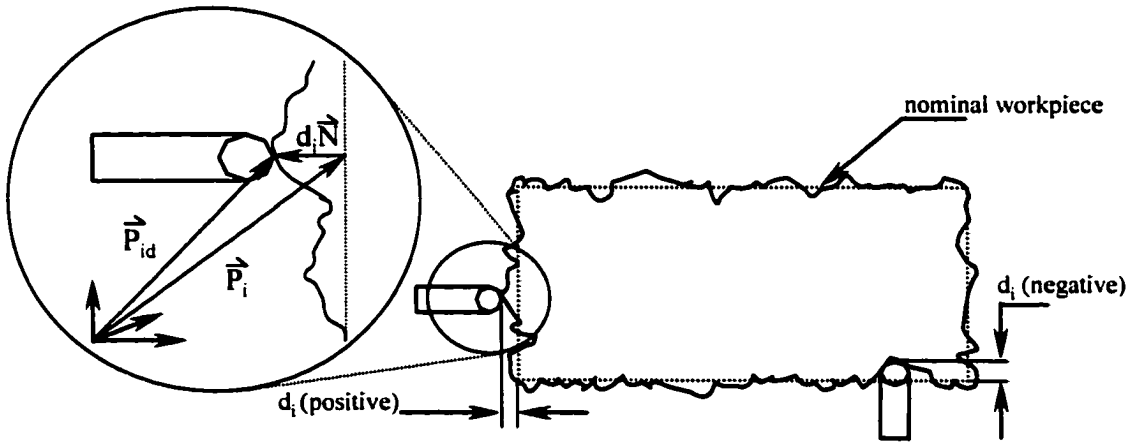

Figure 2. Surface error, its measurement and the relationship between P_i and P_{id}.

GEOMETRIC ANALYSIS

In this paper, the workpiece is virtually brought into contact with the fixture by using a step-wise process, simplified from that developed by Salisbury and Peters [1]. An algorithm was established to find the final orientation and location of the workpiece as affected by the surface errors. Workpiece orientation is represented by two vectors: normal

vectors of the workpiece's primary and secondary planes. A target point, which signifies the workpiece location, could be any crucial point in which we desire to know the variability of its location after fixturing. The target point could be the reference point of a feature to be produced. Throughout this paper, any reference to the primary, secondary and tertiary planes will be referred to as those of the workpiece, unless otherwise stated. The details of the algorithm are described in Appendix I. Note that, the workpiece movements used here are not physical but simulated. However, the result of these simulated moves is the same as actually occurs.

STATISTICAL ANALYSIS

The model in Appendix A was developed to acquire the location of the target point and orientation of the workpiece as a result of surface errors at contact points. Earlier work on this subject only considered a static amount of error, typically the worst-case scenarios. To be more realistic, variable nature of the surface errors will be taken into account here. Such variability is believed to be influential on the location and orientation of the fixtured workpiece. This section will consider the integration of variable error into the model described in the appendix. To evaluate how the variability of the surface errors reflects on that of the workpiece, multivariate and mathematical statistical methods are used. First of all, random numbers denoting surface errors at the locators are generated based on the given distributions. In this paper, a case is presented to use normal distributions.

The mathematical expectation of the distribution of a random variable is called the moment of a random variable. The r^{th} moment about the origin of a random variable X when $y(x)$ is continuous is

$$\mu_r' = \int_{-\infty}^{\infty} x^r y(x)dx \qquad (1)$$

where μ_1' is the mean of the distribution of X, which can be simply denoted by μ. The other special moment used to describe the shape of the distribution of a random variable is the r^{th} moment about the mean.

$$\mu_r = \int_{-\infty}^{\infty} (x-\mu)^r y(x)dx \qquad (2)$$

where μ_2 is the variance of the distribution of X denoted by σ^2.

If closed forms of the equations are not available, or the response function $y(x)$ is too complicated to solve, methods of estimating moments [17-20] can be used to lessen the difficulties in computation. In this paper, the Taylor series approximations and Monte Carlo simulations were implemented and the results from both methods were compared. Using the Taylor series approximation, the downside is the complication of the partial derivatives of the function, which may require some nontrivial algebraic manipulation [20]. Alternatively, Monte Carlo simulation is simpler and more popular for nonlinear statistical analysis, but requires very large samples with low variance in order to obtain accurate estimates of the moments [17, 20, 21].

APPROXIMATION BY TAYLOR SERIES

The surface errors at the locators d_i are assumed to be normally distributed, with a mean of μ_i and a variance of σ_i^2, or $d_i \sim N(\mu_i, \sigma_i^2)$ for i =1,2,..6. According to the algorithm discussed in Appendix A, the final location and orientation of the workpiece in a fixture are nonlinear functions of variables ($d_1, d_2,..,d_6$).

$$\bar{N}'_p = g(d_1, d_2, d_3) \tag{3}$$

$$\bar{N}''_s = h(d_1, d_2, ..., d_5) \tag{4}$$

$$\bar{o}_t = f(d_1, d_2, ..d_6) \tag{5}$$

Johnson and Wichern [22] showed that when $[X_1, X_2, ..., X_n]$ is distributed as MVN($[\mu], \sigma(X_1, X_2, .., X_n)$), any linear combination of X,

$$AX + C = \begin{bmatrix} a_{11}X_1 + & a_{12}X_2 + & \cdots & + a_{1n}X_n \\ a_{21}X_1 + & a_{22}X_2 + & \cdots & + a_{2n}X_n \\ \vdots & \vdots & \vdots & \vdots \\ a_{p1}X_1 + & a_{p2}X_2 + & \cdots & + a_{2n}X_n \end{bmatrix} + \begin{bmatrix} C_1 \\ C_2 \\ \vdots \\ C_p \end{bmatrix} \tag{6}$$

is distributed as a multivariate normal distribution or

$$\text{MVN}(A\mu + C, A\sigma(X_1, X_2, .., X_n)\, A') \tag{7}$$

The response functions in Eq. (3-5); however, are nonlinear as they are derived through a set of complicated equations. Expanding the functions into a Taylor series is suggested. In general, the nonlinear response function $y(x)$ can be approximated by using an extended Taylor series expansion up to the sixth order as follows, according to [17, 20].

$$\begin{aligned} Y \approx f(\mu_1, \mu_2, .. \mu_n) + \sum_a (X_a - \mu_a) f_a + \frac{1}{2!} \sum_{ab} (X_a - \mu_a)(X_b - \mu_b) f_{ab} + .. \\ + \frac{1}{5!} \sum_{abcde} (X_a - \mu_a)(X_b - \mu_b)(X_c - \mu_c)(X_d - \mu_d)(X_e - \mu_e) f_{abcde} + O[(X - \mu)^6] \end{aligned} \tag{8}$$

where f_a, f_{ab} are partial derivatives of f with respect to X_i which is evaluated at $X_t = \mu_t$. The last term of Eq. (8) is negligible terms of sixth order and higher.

The variability of the errors at six locators is small enough to apply only the first order of the Taylor series. The disadvantage of this method is that the Taylor series will only provide accurate results within a limited range. The discrepancy between the Taylor series

approximation and the response function becomes more obvious as the distribution spans over a larger range.

Linearizing Eq. (A.5), (A.18), and (A.27),

$$\bar{N}'_p(\delta) = g(M_3) + [\delta_3 - M_3][\frac{\partial g}{\partial M_3}] \tag{9}$$

$$\bar{N}''_s(\delta) = h(M_5) + [\delta_5 - M_5][\frac{\partial h}{\partial M_5}] \tag{10}$$

$$\bar{o}_t(\delta) = f(M_6) + [\delta - M_6][\frac{\partial f}{\partial M_6}] \tag{11}$$

where M_n = a set of $\mu_1,..., \mu_n$ and δ_n = a set of $d_1,..., d_n$ and $[\delta_n - M_n] = \begin{bmatrix} d_1 - \mu_1 \\ d_2 - \mu_2 \\ \vdots \\ d_n - \mu_n \end{bmatrix}$

By substituting parameters from Eq. (9-11), $(\frac{\partial f}{\partial M_6}), (\frac{\partial g}{\partial M_3})$ and $(\frac{\partial h}{\partial M_5})$ as A, and $f(M_6)$, $g(M_3)$ and $h(M_5)$ as C into Eq. (6), $\bar{o}_t, \bar{N}'_p$, and $\bar{N}''_s$ are distributed as

$$\bar{N}'_p \sim \text{MVN}(g(M_3), (\frac{\partial g}{\partial M_3})\sigma(\delta_3)(\frac{\partial g}{\partial M_3})') \tag{12}$$

$$\bar{N}''_s \sim \text{MVN}(h(M_5), (\frac{\partial h}{\partial M_5})\sigma(\delta_5)(\frac{\partial h}{\partial M_5})') \tag{13}$$

$$\bar{o}_t \sim \text{MVN}(f(M_6), (\frac{\partial f}{\partial M_6})\sigma(\delta_6)(\frac{\partial f}{\partial M_6})') \tag{14}$$

where

$$\sigma(M_n) = \begin{bmatrix} \sigma_{d_1}^2 & \sigma(d_1, d_2) & \cdots & \sigma(d_1, d_n) \\ & \sigma_{d_2}^2 & \cdots & \sigma(d_2, d_n) \\ & & \ddots & \vdots \\ sym & & & \sigma_{d_n}^2 \end{bmatrix} \tag{15}$$

In summary, we can see that the variability of the target point, representing the workpiece location and the normal vectors of the workpiece primary and secondary plane, representing the workpiece orientation, are functions of the partial derivative of the response functions with respect to the surface errors.

APPROXIMATION BY MONTE CARLO SIMULATION

Simulation becomes a choice when the problem cannot be solved for exact solutions, such as the following: [22]

1. Data is either extremely expensive or impossible to obtain.
2. The system or model is so complex that it cannot be described analytically.
3. The model can be explained analytically, but the derivation of the solutions is not straightforward.

Monte Carlo simulations are distinct from other methods since it is neither subject to statistical independence nor is it restricted to a specific type of probabilistic distribution. Despite such simplicity, computational intensity still exists because a large sample size with low variance is required to assure accurate results. Another drawback is that whenever the distributions of the variables change, random numbers must be regenerated and the whole simulation procedure needs to be repeated.

RESULTS

This section is composed of 2 principal subsections: the analysis of the distribution and the comparative numerical results obtained from Monte Carlo simulation and Taylor series approximation. Before the moments can be calculated, multivariate statistical methods will be used to determine the distribution of the data.

RESULTS FROM TAYLOR SERIES APPROXIMATION

By definition, Eq. (12-14) suggest that the distribution of the target point locations and the orientation of the workpiece are multivariate normal distributions associated by parameters shown in the following equations.

$$\bar{N}'_p \sim \mathbf{MVN}(\mu_p, \Sigma_p) \tag{16}$$

$$\bar{N}''_s \sim \mathbf{MVN}(\mu_s, \Sigma_s) \tag{17}$$

$$\bar{o}_t \sim \mathbf{MVN}(\mu_o, \Sigma_o) \tag{18}$$

where Σ_p, Σ_s, and Σ_o are covariance matrices associated in the orientation of the primary and secondary planes, and the location of the workpiece, respectively.

RESULTS FROM MONTE CARLO SIMULATION

Unlike with the Taylor series approximation, distribution assessment of random numbers generated from Monte Carlo simulation is not straightforward. To do so, there are three major steps to perform. For each variable or error at each locator, a random number is created based on a type of statistical distribution assigned by a designer. To obtain the workpiece location and orientation, such random numbers are combined through Eq. (A.5), (A.18) and (A.27). These two steps are repeated until the data generated from the random

numbers is large enough. Deciding how large the sample size would be is sometimes subjective. Accurate results may not be achieved upon an insufficient sample size; however, a large sample size may be redundant and would require extra time and effort to analyze. A sample size of 2500 was used in this study, and is considered adequate because it clearly reveals the shape of the prospective distribution. After the set of the data is created, the moments of the distributions are determined by using standard statistical methods.

DISTRIBUTION OF WORKPIECE LOCATION

In this section, the results from the Monte Carlo simulation based on 2500 samples will be presented. The nominal values of workpiece location and workpiece orientation, which is signified by the normal vector of the primary and secondary plane, are shown in Table 1. The normally distributed data represented surface errors at six contact points were generated by a computer. The means and variances from each distribution are selected to include a combination of negative and positive errors. The unit of the data used throughout this project is millimeter.

Table 1. The nominal values of the target point and workpiece orientation.

variables	nominal value
$\vec{o}$	[25.00 25.00 0]
$\vec{N}_p$	[0 0 1]
$\vec{N}_s$	[1 0 0]

The errors at six contact points here are randomly generated based on a variety of distributions which are expected to be found in reality. We assume that the distributions of the errors in the same plane are alike. For example, the errors at the contact points 1, 2 and 3 are normally distributed with the similar means and variances because these three contact

points are located in the same plane. The moments of the distributions of the errors at 6 locators are tabulated in Table 2.

Table 2. The moments of surface errors. ([a] the means of the distributions and [b] the variances).

Data Set	d_1	d_2	d_3	d_4	d_5	d_6
1	0.0011[a] 0.2553[b]	0.0095 0.2470	-0.0055 0.2564	0.0031 0.0397	-0.0005 0.0387	0.0029 0.0924
2	-0.0049 0.0412	-0.0087 0.0391	-0.0012 0.0392	-0.0027 0.2522	-0.0192 0.2567	-0.0071 0.0910
3	0.0031 0.2463	-0.0231 0.2604	0.0202 0.2502	0.0053 0.0929	0.0059 0.0890	0.0011 0.0406
4	0.0043 0.0394	-0.0028 0.0407	-0.0039 0.0395	-0.0031 0.0850	0.0080 0.0906	-0.0128 0.2612
5	-0.0010 0.0922	0.0100 0.0943	0.0047 0.0894	-0.0056 0.2460	0.0073 0.2487	0.0010 0.0410
6	-0.0027 0.0917	0.0010 0.0933	0.0062 0.0869	0.0033 0.0389	-0.0007 0.0387	-0.0111 0.2552

The procedure of assessing the distribution of the workpiece location begins with an analysis on scatter plots (Figures 3(a-d)). Since the workpiece location is composed of 3 components, the projected location onto x, y and z axes, the plots of x-y, x-z, y-z, and x-y-z are investigated to see if systematic patterns of any distribution present. According to [22], if the data are distributed as a multivariate normal distribution, each bivariate distribution must be normal and the contours of constant density would have elliptical or circular shape. The elliptical clouds exhibited in Figures 3(a-d) suggest a normal distribution. In 3-dimensional system; however, it does not guarantee the global multivariate normal relationship among the three variables. To evaluate the distribution of multivariate data, the normality test is performed by constructing a chi-square plot (see detail in [21]).

To construct the chi-square plot

1.Calculate squared distances $D_j^2 = (x_j - \bar{x})' S^{-1} (x_j - \bar{x})$, where $j = 1,2,..n$ and S is a covariance matrix

2.Order the squared distances from smallest to largest as $D_{(1)}^2 \le D_{(2)}^2 \le \ldots \le D_{(n)}^2$

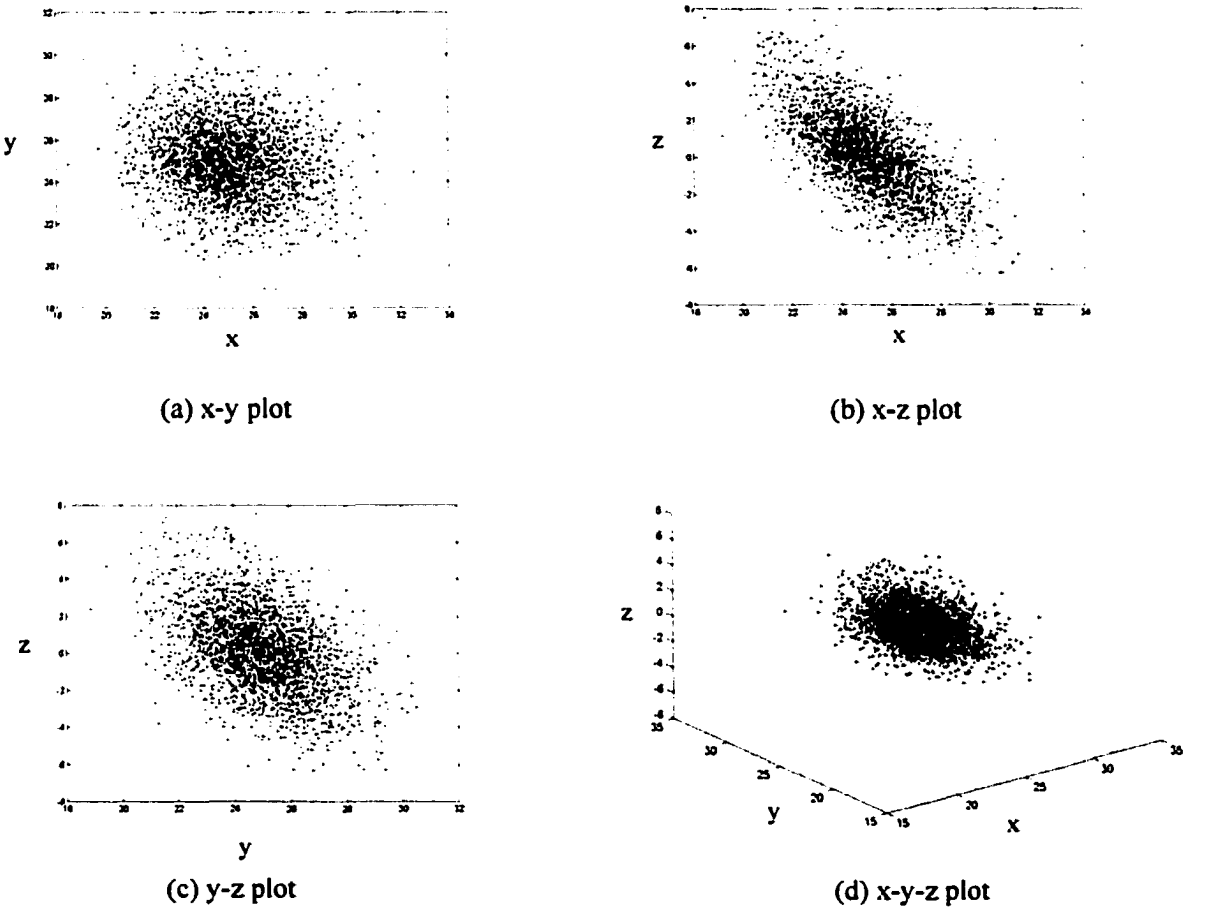

(a) x-y plot

(b) x-z plot

(c) y-z plot

(d) x-y-z plot

Figure 3. The scatter plots of the workpiece location.

3.Graph the pairs $(q_{c,p}(\frac{j-\frac{1}{2}}{n}), D^2_{(j)})$, where $q_{c,p}(\frac{j-\frac{1}{2}}{n})$ is the $100(\frac{j-\frac{1}{2}}{n})$ quantile of the chi-square distribution with p degrees of freedom. In particular,

$$q_{c,p}(\frac{j-\frac{1}{2}}{n}) = \chi^2_p(\frac{n-j+\frac{1}{2}}{n}).$$

If the data are drawn from a multivariate normal distribution, the plot should be similar to a straight line through the origin with slope equal to one. Any systematic curves indicate lack of normality and points far from the line suggest outlying observations. The data were plotted in Figure 4, which strongly indicate that the workpiece location is a multivariate normal distribution.

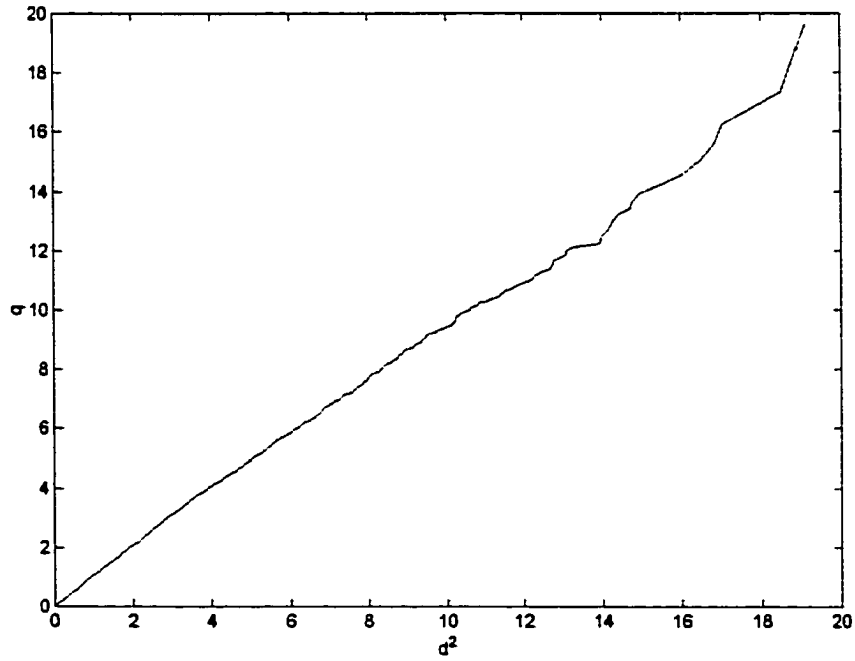

Figure 4. The normality plot of the workpiece location.

DISTRIBUTION OF WORKPIECE ORIENTATION

Since the workpiece orientation is denoted by the combination of the primary and secondary plane orientation, the evaluation of its distribution is therefore based on two separate behaviors of the associated planes. The variability of a plane can be regarded as that of its unit normal vector. Figures 5(a-d) are the plots showing the orientation distribution of the primary plane. These plots indicate the negligible variability along z axis as compared to those in the x and y axes. We will consequently consider the variability of the primary plane orientation as if it is 2-dimensional. When the variability in z axis is ignored, the distribution of the primary plane is evidently bivariate normal distributed, see Figure 5(a).

Similar to the analysis on the distribution of the primary plane, for the secondary plane we will consider only the bivariate distribution between the data in y and z axes since the variability in x direction is extremely small. In Figure 6(c), the normality pattern is clearly presented.

NUMERICAL RESULTS

The results from the Taylor series approximations and the Monte Carlo simulations strongly support the conclusion that the resultant distributions of workpiece location and orientation, which are functions of normally distributed surface errors, are as well normal distributions. The shape of the distribution of workpiece distribution with 3 variables can be simply pictured as a football with the mean of the distribution located at the centroid of the ellipse. Note that, the mean value of the resultant distribution could be slightly different from the nominal workpiece location or orientation as a result of the shift of surface error

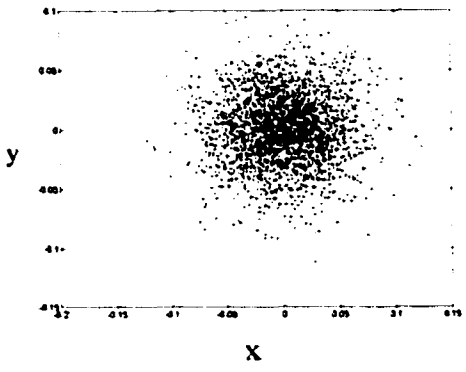

(a) x-y plot

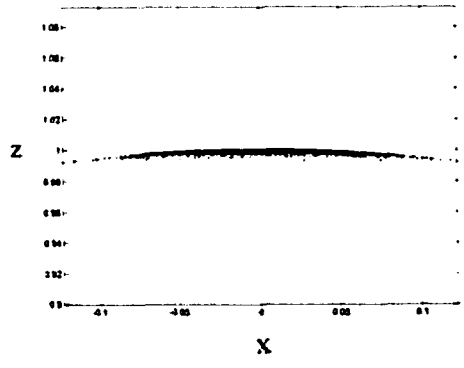

(b) x-z plot

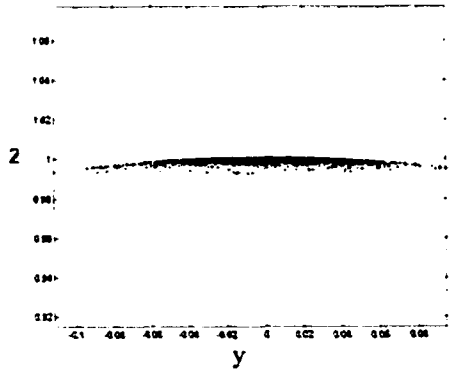

(c) y-z plot

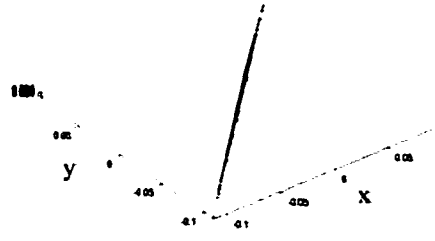

(d) x-y-z plot

Figure 5. The scatter plots of the primary plane orientation.

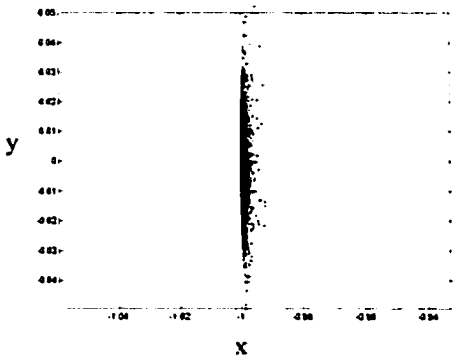

(a) x-y plot

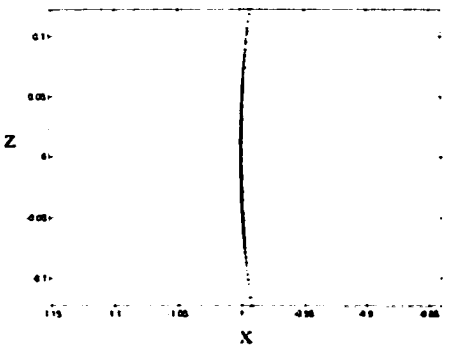

(b) x-z plot

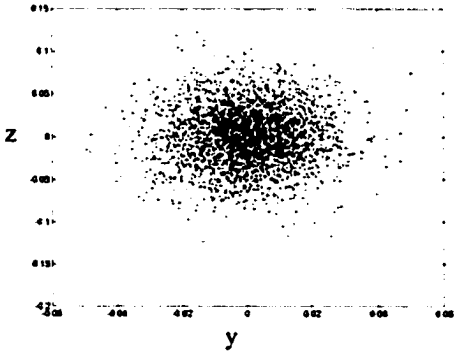

(c) y-z plot

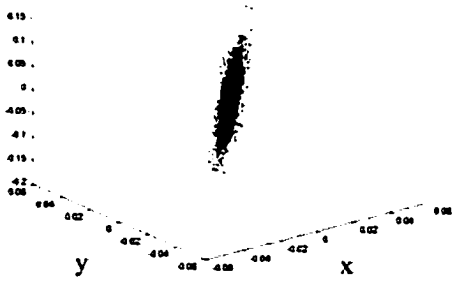

(d) x-y-z plot

Figure 6. The scatter plots of the secondary plane orientation.

means from their nominal values. However, once the means of the surface errors correspond to the nominal values and all of the errors take on their means, the workpiece will be located right at its theoretical position. The distribution (or shape of the football) is controlled by the variances and covariances among the x, y and z coordinates of workpiece location and orientation. Also note that, the distributions of workpiece location and orientation are dependent to each other since they are resulted from the same set of surface errors. It is of interest to see how the variability of the surface errors in each plane contributes to the displacement and variability of workpiece location and orientation. To achieve this goal, we will use the volume of the distribution to quantify the variability of the workpiece location and orientation.

According to [21], the volume of the ellipsoid of probability 1-α, for which the number of the variables greater than 2, is given by

$$V = C * |\Sigma|^{1/2} \tag{19}$$

where Σ is a variance-covariance matrix and C is a constant given by

$$C = \frac{2\Pi^{n/2}}{n\Gamma(\frac{n}{2})}(\chi_n^2(\alpha))^{n/2} \tag{20}$$

where Γ is a gamma function and χ_n^2 is a chi-square function with n degrees of freedom

Since the volume of a $N_n(\mu,\Sigma)$ distribution is proportional to $|\Sigma|^{1/2}$ or a generalized variance, we will use only the second term of Eq. (19) to analyze the effect of variability of surface errors in each plane on the variability of the workpiece location and orientation. Table 3, 4 and 5 contain comparative results from Taylor series approximation and Monte Carlo simulation for each data set.

Table 3. The results from both methods for the workpiece location.

Data Set	Taylor Series Approximation		Monte Carlo Simulation	
	Mean	$\|\Sigma\|^{1/2}$	Mean	$\|\Sigma\|^{1/2}$
1	[25.0132 24.9828 0.0023]	0.2288	[25.0278 24.9815 0.0199]	0.2307
2	[25.0018 24.9964 –0.0059]	0.1383	[25.0160 24.9961 –0.0031]	0.1368
3	[24.9787 25.0297 0.0012]	0.2493	[24.9953 25.0285 0.0187]	0.2480
4	[24.9843 25.0193 0.0101]	0.1012	[24.9907 25.0190 0.0129]	0.1023
5	[24.9990 25.0120 –0.0066]	0.1932	[25.0157 25.0116 –0.0005]	0.1884
6	[25.0090 25.0141 –0.0081]	0.1269	[25.0156 25.0137 –0.0017]	0.1258

Table 4. The results from both methods for the primary plane orientation.

Data Set	Taylor Series Approximation		Monte Carlo Simulation	
	Mean	$\|\Sigma\|^{1/2}$	Mean	$\|\Sigma\|^{1/2}$
1	[-0.0002 0.0002 1.0000]	1.75e-4	[-0.0002 0.0002 0.9998]	1.76e-4
2	[0.0002 –0.0001 1.0000]	2.75e-5	[0.0001 –0.0001 1.0000]	2.72e-5
3	[0.0005 –0.0006 1.0000]	1.74e-4	[0.0005 –0.0006 0.9998]	1.75e-4
4	[0.0001 0.0001 1.0000]	2.76e-5	[0.0001 0.0001 1.0000]	2.80e-5
5	[-0.0002 0 1.0000]	6.37e-5	[-0.0002 0 0.9999]	6.24e-5
6	[-0.0001 –0.0001 1.0000]	6.27e-5	[-0.0001 –0.0001 0.9999]	6.24e-5

Table 5. The results from both methods for the secondary plane orientation.

Data Set	Taylor Series Approximation		Monte Carlo Simulation	
	Mean	$\|\Sigma\|^{1/2}$	Mean	$\|\Sigma\|^{1/2}$
1	[-1.0000 –0.0001 –0.0002]	7.94e-5	[-0.9999 –0.0001 –0.0002]	7.95e-5
2	[-1.0000 –0.0003 0.0001]	8.08e-5	[-0.9999 –0.0003 0.0001]	7.86e-5
3	[-1.0000 0 0.0005]	1.21e-4	[-0.9999 0 0.0005]	1.18e-4
4	[-1.0000 0.0002 0.0001]	4.74e-5	[-0.9999 0.0002 0.0001]	4.81e-5
5	[-1.0000 0.0003 –0.0002]	1.21e-4	[-0.9999 0.0003 –0.0002	1.18e-4
6	[-1.0000 –0.0001 –0.0001]	4.79e-5	[-0.9999 –0.0001 –0.0001]	4.84e-5

CONCLUSION

The results indicate that the discrepancies between the moments estimated from Taylor series approximation and Monte Carlo simulation are not significant. Both methods will provide accurate solutions under different limitations as mentioned previously. Taylor series is recommended whenever the variability of the variables is not large and calculating for partial derivatives is not time consuming. Alternatively, Monte Carlo simulation is much simpler but requires large sample sizes to assure accurate results, and higher computational effort.

It is unlikely to fabricate a geometrically and dimensionally perfect workpiece. As presented in this paper, once the workpiece is set in a fixture the location and orientation of the workpiece are displaced by surface errors at contact points. Being aware of variability of location and orientation of the workpiece would help in tolerancing and fixture design.

REFERENCES

1.Salisbury, E.J. and F.E. Peters, *The impact of surface errors on fixtured workpiece location and orientation.* NAMRC Transactions, 1998. **26**: p. 323-328.

2.Brost, R.C. and K.Y. Goldberg, *A complete algorithm for designing planar fixtures using modular components.* IEEE Transactions on Robotics and Automation, 1996. **12**: p. 31-45.

3.Cai, W., S.J. Hu, and J.X. Yuan, *A variational method of robust fixture configuration design for 3-d workpieces.* Journal of Manufacturing Science and Engineering, 1997. **119**: p. 593-602.

4.Cai, W., S.J. Hu, and J.X. Yuan, *Deformable sheet metal fixturing:principles, algorithms and simulations.* Journal of Manufacturing Science and Engineering, 1996. **118**: p. 318-324.

5.King, L.S.-B. and I. Hutter, *Theoretical approach for generating optimal fixturing locations for prismatic workparts in automated assembly.* Journal of Manufacturing Systems, 1993. **12**: p. 409-416.

6.Trappey, J.C. and S. Matrubhutam, *Fixture configuration using projective geometry.* Journal of Manufacturing Systems, 1993. **12**: p. 486-495.

7.Wu, Y., et al., *Automated modular fixture planning geometric analysis.* Robotics and Computer-integrated Manufacturing, 1998. **14**: p. 1-15.

8.Fuh, J.Y.H., C.-H. Chang, and M.A. Melkanoff, *An integrated fixture planning and analysis system for machining processes.* Robotics and Computer-integrated Manufacturing, 1993. **10**: p. 339-353.

9.DeMeter, E.C., *Restraint analysis of fixtures which rely on surface contact.* Journal of Engineering for Industry, 1994. **116**: p. 207-15.

10.DeMeter, E.C., *The min-max load criteria as a measure of machining fixture performance.* Journal of Engineering for Industry, 1994. **116**: p. 500-507.

11.DeMeter, E.C., *Min-max load model for optimizing machining fixture performance.* Journal of Engineering for Industry, 1995. **117**: p. 186-193.

12.Hockenberger, M.J. and E.C. De-Meter, *The application of meta functions to the quasi-static analysis of workpiece displacement within a machining fixture.* Journal of Manufacturing Science and Engineering, 1996. **118**: p. 325-31.

13.Rong, Y. and Y. Bai, *Machining accuracy analysis for computer-aided fixture design verification.* Journal of Manufacturing Science and Engineering, 1996. **118**: p. 289-300.

14.Ong, S.K. and A.Y.C. Nee, *A systematic approach for analyzing the fixturability of parts for machining.* Journal of Manufacturing Science and Engineering, 1998. **120**: p. 401-407.

15.Choudhuri, S.A. and E.C. De-Meter, *Tolerance analysis of machining fixture locators.* Journal of Manufacturing Science and Engineering, 1999. **121**: p. 273-81.

16.Sangnui, S. and F.E. Peters, *The impact of surface errors on the location and orientation of a cylindrical workpiece in a fixture.* Journal of Manufacturing Science and Engineering, 2001. **123**.

17.Evans, D.H., *Statistical tolerancing: the state of the art, pt. 2 methods for estimating moments.* Journal of Quality Technology, 1975.

18.Evans, D.H., *An application of numerical integration techniques to statistical tolerancing.* Technometrics, 1967. **9**(3): p. 441-456.

19.Evans, D.H., *An application of numerical integration techniques to statistical tolerancing, III General distributions.* Technometrics, 1972. **14**(1): p. 23-35.

20.Nigam, S.D. and J.U. Turner, *Review of statistical approaches to tolerance analysis.* Computer Aided Design, 1995. **27**(1): p. 6-15.

21.Nassef, A.O. and H.A. ElMaraghy, *Statistical analysis and optimal allocation of geometric tolerances.* Proceedings of the 1995 Database Symposium, ASME Database Symposium, 1995: p. 817-824.

22.Johnson, R.A. and D.W. Wichern, *Applied Multivariate Statistical Analysis.* 4 ed. 1998, Upper Saddle River, NJ: Prentice-Hall, Inc.

23.Kalpakjian, S., *Manufacturing Processes for Enigneering Materials.* 2nd ed. 1991: Addison-Wesley Publishing Company, Inc.

CHAPTER 3. DETERMINATION OF APPROPRIATE TOLERANCES OF MACHINE FEATURES WHEN THERE ARE SURFACE ERRORS AT THE FIXTURING POINTS

A paper to be submitted to the Journal of Manufacturing Science and Engineering

Supapan Sangnui and Frank E. Peters

ABSTRACT

The objective of this study is to show the impact of the variability in workpiece location and orientation to feature tolerancing. A feature is fabricated to the workpiece, and its location and orientation will be studied. Because of an inconsistency in location and orientation of the workpiece coordinate system with respect to the machine coordinate system, variability in feature position and orientation is expected. In this work, the workpiece will be assumed to sit at its nominal location and orientation. Instead of modeling transformation to the workpiece, an equivalent transformation is applied to the cutter. Multivariate statistical analysis will be applied to figure the contour of the distribution. Once the distributions of feature position and orientation are known, circular variation region, which occupies the desired probability of acceptance, can be achieved through statistical methods [13-22].

LIST OF SYMBOLS

Σ	variance-covariance matrix
Σ_p	variance-covariance matrix of the hole position
μ	mean of the distribution
μ_p	mean of the distribution of the hole position
σ_i	standard deviation of i^{th} variable
σ^2_i	variance of i^{th} variable
ρ_{ij}	correlation coefficient of i^{th} and j^{th} variables
T	transformation matrix
ϕ	angle of rotation
u	axis of rotation
P	hole position
N	normal vector of the plane or the direction cosine of the hole axis
P_w	nominal position of the hole in the workpiece ref. system
Q_w	actual position of the hole in the workpiece ref. system
P_f	nominal position of the hole in the fixture ref. system
Q_f	actual position of the hole in the fixture ref. system
L	length of the hole
e	eigenvector
λ	eigenvalue
R	radius of the circular variation region
N_p	normal vector to the workpiece primary plane
N_c	direction cosine of the hole
P_p	location of the workpiece primary plane
P_c	virtual location of the hole
O	true location of the hole
Q	point of intersection between the workpiece primary plane and the hole axis

INTRODUCTION

For most applications, it would be possible but infeasible to map a part coordinate system with that of a machine. This inconsistency results in variation in part location and orientation relative to the machine coordinate system, and probably threatens accuracy of a feature which is subject to be made on such part. Earlier, the authors investigated the impact of surface errors at contact points on the deviation in position and orientation of a fixtured workpiece. A relationship between the distribution of surface errors and the resultant distributions of the workpiece location and orientation was established. In this paper, implementing quantitative knowledge of the part displacement, the authors are able to analyze the variation of a component feature. A method to define a geometric variation zone of the feature in relation to the part displacement is presented. This zone is equivalent to a tolerance zone except that it is constructed based on an actual variation of the feature, while the tolerance zone is an allowable zone specified by a designer.

Although there are several factors taking part in establishing tolerance of machined features, understanding how feature variation is affected by the inconsistency existing between the systems of the part and of the machine would help improve the end product accuracy. Once the variation of the original part is known, by implementing the method developed here manufacturers would be able to create higher quality products through imposing more appropriate tolerances, modifying the cutting tool path to compensate these variable part properties or improving the fixture. This paper introduces a new aspect which would make the mechanics of tolerancing more functional.

STATISTICAL TOLERANCING

Many tolerancing methods have been proposed to control variability in manufacturing. However, conventional tolerancing that we are using nowadays is inadequate to represent the variability of manufacturing parts for some reasons as follows [5].

1. Conventional methods treat the tolerances as limits on the parameters of a parametric model. However, as geometric tolerancing represented by tolerance zones instead of limits is more widely accepted, conventional methods become more awkward.

2. In assembly, tolerances that are built up from either worst-case methods or root-sum-squares method are not accurate. Worst-case methods give results that are overly pessimistic, while the root-sum-squares method gives results that are too optimistic.

Because of the above reasons, statistical tolerancing seems to be a choice to bridge the gap between variability in dimension and geometry of manufacturing parts and geometric tolerancing. Statistical tolerancing is a way to allocate tolerances by using probabilistic model to explain variable nature of the parts. Having advantages over the conventional tolerancing, both statistical and geometric tolerancing are becoming industry standard. It is important to explain geometric tolerance statistically. However, the distribution which best describes the variability in manufacturing is controversial. Despite some opposition [7, 8], many researchers [4-6] use a normal or Gaussian distribution to represent the variability. If the event of interest randomly occurs and the sample size is large enough, a normal distribution seems to be an excellent candidate. Even though the sample is not random, we can still theoretically assume a normal distribution with a large sample size by following the central limit theorem. Therefore, a normal distribution is adopted in the first part of this paper to denote the variable nature of surface errors.

Multivariate analysis has been used to explain problems which are under control of several parameters, since they are mathematically tractable and a nice result can be obtained

[11], for many applications. Multivariate normal distributions will be used to describe our fixturing models. Unlike a univariate normal distribution where the probability is represented by the area under the bell-shaped curve, probability of the multivariate distribution is represented by volumes under the surface over regions defined by intervals of the x_i values. The equation of multivariate normal distribution with n parameters is presented in Eq. (1).

$$f(x)=\frac{1}{(2\Pi)^{n/2}|\Sigma|^{1/2}}e^{-(x-\mu)'\Sigma^{-1}(x-\mu)/2} \qquad (1)$$

where $-\infty < x_i < \infty$, $i = 1,2,..,n$, Σ is a variance-covariance matrix and $x=\begin{bmatrix} x_1 \\ x_2 \\ \vdots \\ x_n \end{bmatrix}, \mu=\begin{bmatrix} \mu_1 \\ \mu_2 \\ \vdots \\ \mu_n \end{bmatrix}$

When n=2, a bivariate normal distribution is generally explained by the following equation.

$$f(x_1,x_2)=\frac{1}{2\Pi\sqrt{\sigma_1^2\sigma_{12}(1-\rho_{12}^2)}}\exp\{\frac{-1}{2(1-\rho_{12}^2)}[(\frac{x_1-\mu_1}{\sqrt{\sigma_1^2}})^2+(\frac{x_2-\mu_2}{\sqrt{\sigma_2^2}})^2-2\rho_{12}(\frac{x_1-\mu_1}{\sqrt{\sigma_1^2}})(\frac{x_2-\mu_2}{\sqrt{\sigma_2^2}})]\} \qquad (2)$$

where σ_i is a standard deviation of parameter i, σ_i^2 is a variance of parameter i, and ρ_{ij} is a correlation coefficient of parameter i and j.

When x_1 and x_2 are independent, the equation can be simplified by substituting ρ_{12} with 0. In other words, the joint distribution of x_1 and x_2 can be written as a product of two univariate normal densities.

$$f(x_1,x_2)=\frac{1}{2\Pi\sqrt{\sigma_{11}\sigma_{12}}}\exp\{\frac{-1}{2}[(\frac{x_1-\mu_1}{\sqrt{\sigma_{11}}})^2+(\frac{x_2-\mu_2}{\sqrt{\sigma_{22}}})^2]\} \qquad (3)$$

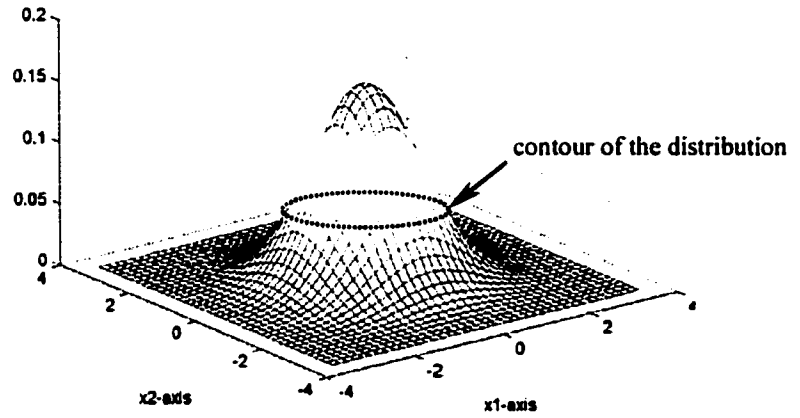

Figure 1. A bivariate normal distribution.

A bivariate normal distribution is pictured in 3-dimensional space as "a hill" and the probability is taken from the volume under the hill within specified ranges of x_1 and x_2, as seen in Figure 1. At a given probability density, there exist points that are equidistant from x_1-x_2 plane forming a single layer of points, which is bounded by various shapes of contours. Investigating the contours is important because it provides us with useful information about characteristics of the distribution. The contours of bivariate normal distributions tend to be elliptical except when $\rho_{12} = 0$ and $\sigma_{x1}=\sigma_{x2}$ as shown in Figure 2. The orientation of the contour mainly depends on σ^2_{x1}, σ^2_{x2} and ρ_{12}, and the location is determined by μ_{x1} and μ_{x2}. Examples of contours of bivariate normal distributions are shown in Figure 2.

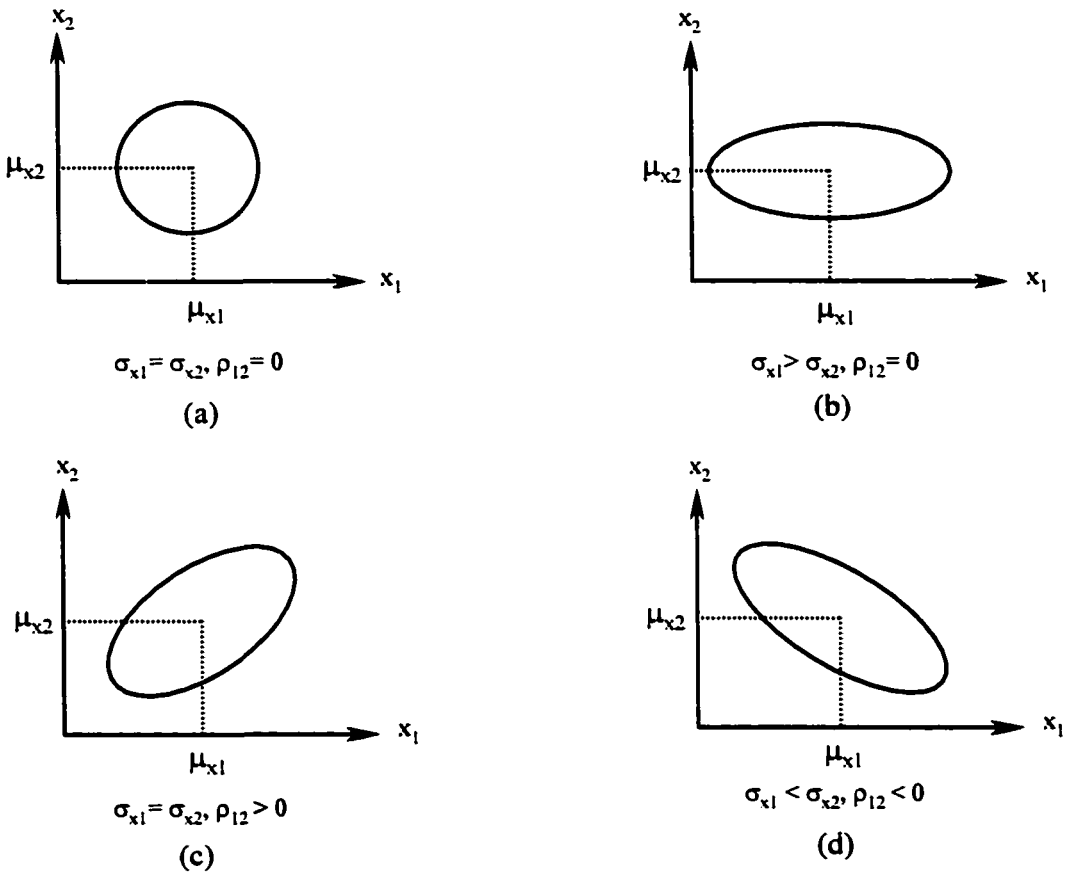

Figure 2. The contour of bivariate normal distributions associated by different variances and correlation between x_1 and x_2.

LITERATURE REVIEW

There are a number of researchers developing algorithms to establish appropriate tolerances for features. Roy and Li [1] investigated a complete form tolerance zone definition based on model variation. The paper proposed two approaches to represent the variant boundary surfaces that approximated the real world form variations and simulated the

variations by planar surfaces. The first approach was to generate random admissible points that would be used to construct curved surfaces, where the latter approach was to construct simulated planar surface, which was corresponding to the randomly generated points. Nevertheless, this model was highly sensitive to a distribution of the random number, which the authors dismissed to discuss in the paper. Later, Roy and Li [2] proposed a procedure to represent size, orientation and position tolerance for polyhedral objects. The variational model was constructed from its nominal boundary model by allowing each of the bounding surfaces to be varied within some specified tolerance zones, and by defining new edges and vertices at the surface intersections. The variational model was established for the size, orientation and position tolerance, then the resultant tolerance was calculated based on the aggregation of tolerances, which were applicable to the surface. Since the surface defined in the paper was planar surface, there were a few parameters controlling the location and orientation of the surface. ElMaraghy et al [3] proposed a mathematical definition for geometric tolerance zones according to the ANSI Y14.5M Geometric Tolerance Standard. The paper included a tolerance analysis of both planar and axis features. The parameters defining a sample space were the parameters used to generate the components. A random number generator, with uniform distribution, was utilized to select sample points within the sample space. Once again, the efficiency of the model seemed to be dependent on the selected distribution of the random parameters. To date, no statistical model has been widely accepted to represent the variability produced in manufacturing. It is almost impossible to choose a single distribution to represent such variability from every process. The nature of the geometrical error tends to vary from process to process or even under the same process the error model can be different upon the parameters of the process change. These

researchers focused on developing variational models, which is claimed to reasonably represent the geometrical variability of objects. In addition, more work has been carried out in the area of imposing tolerances based on the information from CMM or other measuring devices. Hong et al [4] proposed ways to define tolerance zones of straightness and flatness by using simulated annealing. The algorithm employed the geometrical properties obtained from coordinate measuring machines and combines nonlinear optimization with computational geometry. Traband et al [5] presented an algorithm to determine if features meet flatness and straightness requirements according to ASME Y14.5M. The authors used the points measured from CMM to represent geometric properties of the features. The minimum tolerance zone is derived by utilizing convex hull concept.

METHODOLOGY

Geometric tolerancing was developed to overcome three main shortcomings of conventional tolerancing schemes: incapability of conventional methods in controlling all aspects of the shape of a part, exclusion of datum concept, and unsuitability of extending to control locations or angular dimensions [12]. There are five types of geometric tolerances, which are location, orientation, form, profile and runout tolerances (see detail in [13]). Our goal is to provide information needed in establishing more appropriate tolerance of the feature. In this study, a type of positional tolerance applied to a cylindrical feature will be the focus of our investigation. Since orientation tolerance of a cylindrical feature is a part of positional tolerance, it is rarely used unless specifically

needed. As a result, only positional tolerancing of a cylindrical feature will be presented here.

GEOMETRIC ANALYSIS

Suppose that the workpiece is fixtured at $\bar{P}_w$ with respect to the machine reference system in order to drill a hole at $\bar{P}_f$ with respect to the workpiece reference system. However, in a consequence of undesirable factors the workpiece will be displaced to $\bar{P}'_w$ (see Figure 3), while the hole stays at the same position in the machine reference system. This inconsistency causes problems in locating and results in dimensional and geometrical errors of the feature. Not only the position of the hole will be subject to variation, but also its orientation. They are dependent on each other since they both are functions of the same factors.

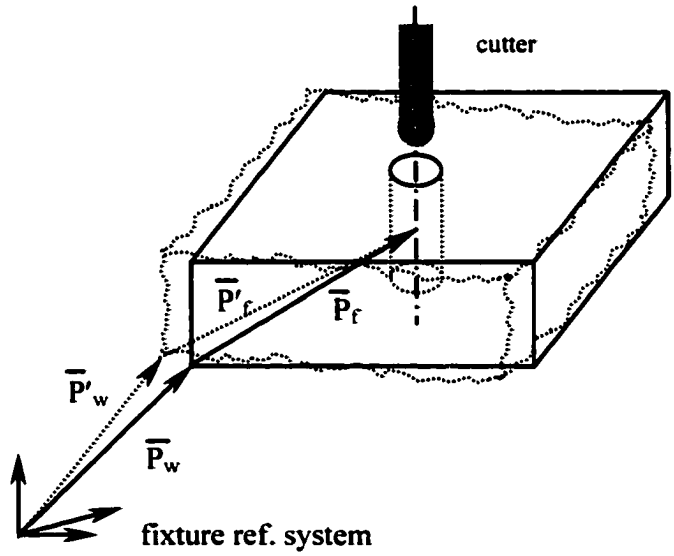

Figure 3. The displacement of the point of interest Qf→Pf

While any point on the workpiece can be used to define its position, for simplicity, we will designate the position of the feature and that of the workpiece to be the same. In this study, the feature position is targeted at the mid point between the top and bottom planes to reduce an angular error caused by variable workpiece orientation. The axis of the feature is thus obtained by projecting the point, which represents the feature position up and down, along the cutting direction onto the top and bottom planes. The projected points on these planes are considered the extreme points or the end points of the potential axes. The geometric variation region representing the variation of the feature, as affected by the variability in workpiece location and orientation, is the zone containing the extreme points. In this section, a method to define the geometric variation region that includes a desired proportion of the extreme points will be presented.

Before the geometric variation region can be defined, the distribution of the projected or extreme points will be evaluated, and the details are illustrated in Appendix B.

STATISTICAL ANALYSIS

Statistical methods are used to evaluate the distribution of the projected or extreme points, and later to find the geometric variation region in relation to the desired probability of acceptance.

TRANSFORMATION OF AN ELLIPSE

The distribution of the projected points is proved in Appendix B to be normally distributed and has ellipse-like contour. It is derived under the influence of correlations between variables. However, the establishment of circular variation regions developed by researchers [14-22] in the later section is valid only when the variables are independently and

normally distributed, or when the ellipse is oriented similar to Figure 2(a) and 2(b). Therefore, appropriate transformation, which makes the structure of the data having such properties, is required. If the mean of the distribution is offset from the origin of the system, or μ_{x1} or μ_{x2} are not zero, the transformation would be translation. Rotation about point (μ_{x1}, μ_{x2}) by θ is needed if the axes of the ellipse do not coincide with the system's axes. The angle, θ, can be obtained from the following equation.

$$\tan 2\theta = \frac{2\rho_{12}\sigma_{x1}\sigma_{x2}}{\sigma_{x1}^2 - \sigma_{x2}^2} \qquad (4)$$

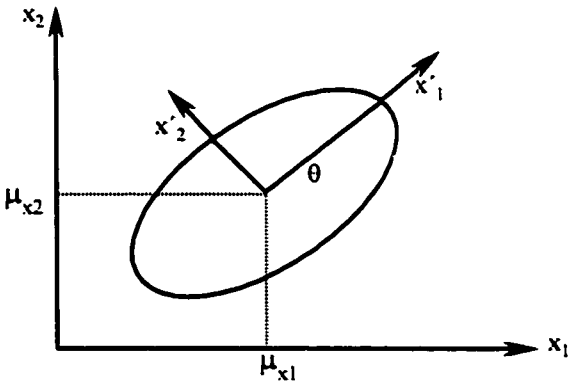

Figure 4. The determination of ellipse in two coordinate systems.

From Figure 4, the ellipse is centered at (μ_{x1}, μ_{x2}) and its axes tilt by θ with respect to x_1-x_2 coordinate system. The ellipse will be rotated clockwise, allowing its major and minor axes to correspond to the axes of the x_1-x_2 frame. It is then translated by [μ_{x1}, μ_{x2}] to the origin of the system. These steps are represented by the following transformation matrix.

$$T = \begin{bmatrix} \cos(\theta) & \sin(\theta) & \mu_{x1} \\ -\sin(\theta) & \cos(\theta) & \mu_{x2} \\ 0 & 0 & 1 \end{bmatrix} \tag{5}$$

After the transformation is achieved, the variances of the newly transformed distribution can be obtained by performing the above calculation backward. As previously stated, the characteristics of the contour are determined by the eigenvalues and eigenvectors of variance-covariance matrix of the population. A change in the orientation of the ellipse results in new eigenvectors, which coincide with the x_1 and x_2 axes (as shown in Figure 5). Let's call the original distribution, A, and the transformed one, B. This means that the eigenvalues of A and B are the same. In the previous section, we have found the variance–covariance matrix of A, and let's name the eigenvalues of this matrix, λ_{A1}, and λ_{A2}.

$$\lambda_A = \lambda_B \tag{6}$$

We know, from Figure 5, that the eigenvectors of B must be v_{B1}=[1 0] and v_{B2}=[0 1]. From the definition of eigenvectors and eigenvalues,

$$\Sigma_B v_B = \lambda_B v_B \tag{7}$$

We also know that the components of B are independent, see Figure 5 compared to Figure 2, so the covariance terms in the variance-covariance matrix of B are zero.

$$\Sigma_B = \begin{bmatrix} \sigma_{B1}^2 & 0 \\ 0 & \sigma_{B2}^2 \end{bmatrix} \tag{8}$$

Substitute Σ_B, v_B and λ_A into Eq.(7) and we derive

$$\sigma_{B1}^2 = \lambda_{A1} \text{ and } \sigma_{B2}^2 = \lambda_{A2} \tag{9}$$

Now, we are ready to find a circle which is concentric with the ellipse and occupies a desired bivariate normal probability.

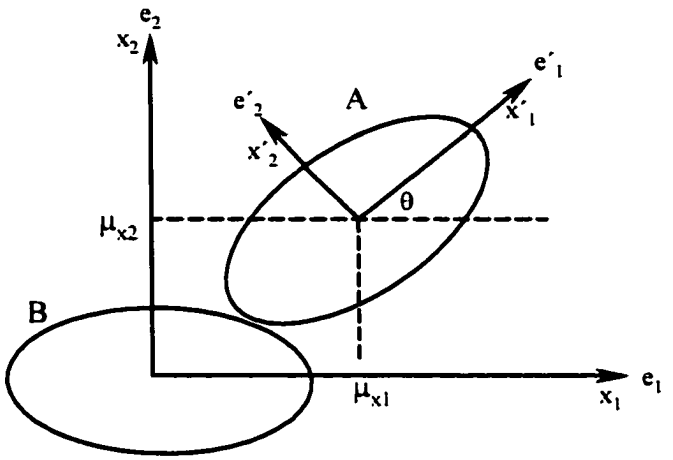

Figure 5. The transformation of the ellipse.

CIRCULAR VARIATION REGION

There are many ways to draw a circle with a specified probability out of the elliptical region of a bivariate normal distribution. Integrating over the region is one choice. However, such high precision would be redundant in practice. Several statisticians [14, 15, 19, 22] made formulas related to a geometric variation region established from a multivariate normal distribution available. The establishment of circular regions, which include a specified fraction of a bivariate normal distribution was developed by E. N. Oberg [21]. He proposed 3 approximate formulas to obtain a radius of the circle, R_{d1}, R_{d2}, and R_{d3}. The first formula is derived from equating the area of a circle of a radius, R_{d1}, to the area of the ellipse, which includes the probability, p. This formula will closely estimate the true R when σ_{B1} is close to σ_{B2}, but will underestimate the true R whenever $\sigma_{B1} \neq \sigma_{B2}$, making it undesirable in some applications. By performing integration over a circular area, R_{d2} of a circle

circumscribing a desired probability is derived. The last formula is obtained by taking the root-mean-square of the former two. It yields better results when $\frac{\sigma_{B1}}{\sigma_{B2}} \geq 0.5$; $\sigma_{B1} \leq \sigma_{B2}$.

Harter [18] employed numerical integration to determine the factor K, which is equal to R/σ_1 when σ_1 is the smaller standard deviation. Lowe [20] used numerical integration to calculate the integral of a bivariate normal distribution. The author provided tables of probabilities of the bivariate normal distribution, which are bounded by the given offset circles. Weingarten and Donato [23], and Gilliland [16] proposed approximate formulas to define a radius of the circle. They then tabulated and compared the results derived from these formulas. Hall and Sheldon [17] published procedures and tables of tolerance regions obtained from the bivariate normal distribution, which was claimed to be the most accurate at the time. Below are the explicit formulas provided in the mentioned papers.

Formulas by E. N. Oberg [21];

$$R_{d1} = \sqrt{2\sigma_{B1}\sigma_{B2} ln(\frac{1}{1-p})} \tag{10}$$

$$R_{d2} = \sqrt{(\sigma_{B1}^2 + \sigma_{B2}^2) ln(\frac{1}{1-p})} \tag{11}$$

$$R_{d3} = (\sigma_{B1} + \sigma_{B2}) \sqrt{\frac{1}{2} ln(\frac{1}{1-p})} \tag{12}$$

Formula by Harter[18];

$R_d = K\sigma_2$ (by calling the larger of the two standard deviation σ_2) (13)

K is dependent on c which is the ratio of σ_1 and σ_2 or $\frac{\sigma_1}{\sigma_2}$. The values of K corresponding to c and the cumulative probability p are tabulated in Harter [18] and also presented below in Table 1. However, when $c = 1$, closed form of K is derived determined by Eq. (14).

$$K = \sqrt{-2\ln(1-p)} \tag{14}$$

Table 1. The values of K obtained from Harter[18].

probability	ratio of σ_1 and σ_2, c					
p	0.0	0.1	0.2	0.3	0.4	0.5
0.5000	0.67449	0.68199	0.70585	0.74993	0.80785	0.87042
0.7500	1.15035	1.15473	1.16825	1.19246	1.23100	1.28534
0.9000	1.64485	1.64791	1.65731	1.67383	1.69981	1.73708
0.9500	1.95996	1.96253	1.97041	1.98420	2.00514	2.03586
0.9750	2.24140	2.24365	2.25053	2.26255	2.28073	2.30707
0.9900	2.57583	2.57778	2.58377	2.59421	2.60995	2.63257
0.9950	2.80703	2.80883	2.81432	2.83289	2.83830	2.85894
0.9975	3.02334	2.02500	3.03010	3.03898	3.05234	3.07144
0.9990	3.29053	3.29206	3.29673	3.30489	3.31715	3.33464

probability	ratio of σ_1 and σ_2, c				
p	0.6	0.7	0.8	0.9	1.0
0.5000	0.93365	0.99621	1.05769	1.11807	1.17741
0.7500	1.35143	1.42471	1.50231	1.58271	1.66511
0.9000	1.79152	1.86253	1.94761	2.04236	2.14597
0.9500	2.08130	2.14598	2.23029	2.33180	2.44775
0.9750	2.34581	2.40356	2.48494	2.58999	2.71620
0.9900	2.66533	2.71515	2.79069	2.89743	3.03485
0.9950	2.88859	2.93347	3.00431	3.11073	3.25525
0.9975	3.09871	3.13969	3.20586	3.31099	3.46164
0.9990	3.35949	3.39647	3.45698	3.55939	3.71692

In addition, Lowe[20] has tabulated the integral of the bivariate normal distribution over an offset circle. Below is a part of the table presented in Lowe's work, which is useful for this study. The numbers in the table represent the probability covered by a circle with radius R. The probability belongs to the bivariate normal distribution with the variances of σ_1 and σ_2 where $\sigma_1 \leq \sigma_2$.

Table 2. The probability of acceptance related to R and σ_1, σ_2 obtained from Lowe[20].

σ_1/σ_2	R/σ_2					
	1	2	4	8	16	32
1	0.393	0.865	1.000	0.999	-	-
2	0.215	0.590	0.945	1.000	-	-
4	0.110	0.325	0.666	0.953	1.000	-
8	0.055	0.167	0.371	0.679	0.954	1.000

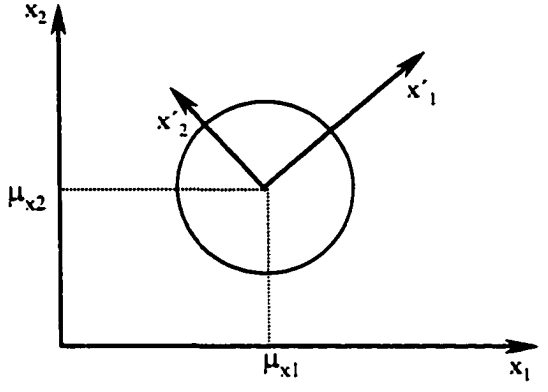

Figure 6. The circular region occupying a certain bivariate normal probability.

From Figure 6, we can see that the circle and the ellipse share the same center point. The radius of the circle is dependent on the desired probability and the variances of the bivariate normal population, according to Eq. (10)-(14). The loss in efficiency in terms of area when using the circular region to represent the ellipse is discussed in Chew [14]. For example, when $\sigma_1 = 0.4788$ and $\sigma_2 = 1.010$, by using Harter's equation in Eq.(13) the radius of the 95% circle is 2.2195, resulting in the area of 3.1587π. Based on the same ellipse, its area is 4.9262π, which is 55.95 % less than the area of the circle. This loss is smaller as the shape of the ellipse is getting closer to a circle. The loss is reduced to 0.88% when the ratio of σ_1 and σ_2 is increased to 0.8981. As previously mentioned, the ellipse contour is

controlled by the eigenvalues of the covariance matrix of the population. It is likely to become a circle when the eigenvalues are close to each other. The term that determines the difference between the eigenvalues is $\sqrt{(\sigma_1^2 - \sigma_2^2)^2 + 4\sigma_{12}^2}$. To minimize the difference,

$$\sigma_1 \approx \sigma_2 \text{ and } \sigma_{12} \approx 0 \qquad (15)$$

Theoretically, the loss in area efficiency is negligible if σ in both directions are approximately the same and the covariance σ_{12} is close to 0. Researchers like Oberg [21] tried to minimize the difference in area between the ellipse and the prospective circle. At the same desired probability, when the correlations among the variables are getting higher, the radius of the circle will be larger, trying to maintain the same probability. The drawback is that the circle tends to include the larger area of zero bivariate normal probability.

RESULTS

The theoretical results presented in this section are obtained by implementing surface errors shown in Table 3, 4 and 5 in the previous chapter. This information represents the variability of workpiece position and orientation, which will be used as input to evaluate geometrical variation of the feature. The characteristics of the feature position based on each set of surface errors are presented in Table 3.

Table 3. The characteristics of the projections.

Data Set	σ_x	σ_y	ρ_{xy}
1	0.5859	0.5574	-0.0595
2	0.7020	0.6335	-0.4869
3	0.7162	0.6022	-0.1910
4	0.2966	0.4945	-0.1653
5	0.7897	0.6518	-0.4866
6	0.2879	0.4679	-0.0873

The last column contains the correlations between the x and y components. It indicates dependency between the variables, which is problematic in determining geometrical variation region. The above distributions are transformed by using Eq. (5) in order to eliminate such correlations. Once the desired distributions were achieved, circular variation regions will be established by using Eq. (10-13) and presented in Table 4. The numbers in the second lines of each row in the first column represent the ratio of σ_1 and σ_2. The percents of the loss of area efficiency are shown under the radiuses of the circular region. When the ratio is close to 1, the radiuses obtained from all four equations are similar. However, whenever the ratio of σ_1 and σ_2 is getting lower, the radiuses in the second column tend to be smaller than the others. It is because the equation which is used to calculate these numbers is subject to equating the area of the ellipse and the circle, but ignores the correlation between the variables.

Table 4. Circular variation regions when $p = 0.95$ derived from Oberg [21] and Harter[18], [a] the ratio of σ_1 and σ_2 where $\sigma_1 < \sigma_2$ and [b] the percent of the loss of area efficiency.

data set	R_{d1}	R_{d2}	R_{d3}	R_h
1	1.8454	1.8507	1.8480	1.8535
(0.8981)[a]	2.74e-3%[b]	0.58%	0.29%	0.88%
2	1.6523	2.0002	1.8345	2.1544
(0.3942)	2.74e-3%	46.54%	23.27%	70.01%
3	1.9403	1.9874	1.9640	2.0133
(0.7319)	2.74e-3%	4.91%	2.46%	7.67%
4	1.4387	1.5395	1.4899	1.5918
(0.5873)	2.74e-3%	14.50%	7.25%	22.42%
5	1.7773	2.0781	1.9335	2.2195
(0.4349)	2.74e-3%	36.71%	18.36%	55.95%
6	1.4615	1.5047	1.4833	1.5274
(0.7083)	2.74e-3%	6.01%	3.01%	9.23%

MODEL VALIDATION

To validate the numerical model, an experiment was conducted using a special fixture and a coordinate measuring machine (CMM.) The workpiece used in this experiment was a prismatic piece (8x4x2 inches) with a 1-inch diameter through hole in the center of the largest plan of the workpiece. This hole was the feature of interest, and its position and orientation during the experiments was measured.

Since the purpose of the experiment was to study the effect of workpiece surface errors on the location and orientation of a workpiece, a method to introduce variability was needed. Instead of using workpieces with variable surface errors and a fixture with locators in fixed positions, the fixture was designed with adjustable locators. Spherical tips were placed on a micrometer body, and fitted onto the fixture. Variable surface errors could be simulated by moving the tips along the direction perpendicular to the workpiece datum surfaces.

The workpiece was supported by six locators, three on the primary plane, two on the secondary plane, and the last one on the tertiary plane. While the workpiece was located in the fixture, its location and orientation were measured by using a CMM Through the information about the workpiece variability, we are able to determine geometrical variation of the feature that would help in establishing component tolerance thereafter.

EXPERIMENTAL PROCEDURES

Normally distributed random numbers representing errors at each locator were generated within variabilty ranges specified in Table 5. The numbers in the table are the

intervals that contain 3σ of random number normal population with means at zero. According to the assumption stated earlier, all of the errors for locators in the same plane shared the similar distribution.

Data Set	Primary Plane	Secondary Plane	Tertiary Plane
1	[-0.0785, 0.0785]	[-0.0785, 0.0785]	[-0.059, 0.059]
2	[-0.118, 0.118]	[-0.118, 0.118]	[-0.0785, 0.0785]
3	[-0.118, 0.118]	[-0.0785, 0.0785]	[-0.0393 0.0393]
4	[-0.197, 0.197]	[-0.1575, 0.1575]	[-0.0785, 0.0785]

Table 5. Variability range applied to each plane (in).

With the micrometers set at their zeros, the location and orientation of the workpiece and the feature were considered nominal. In each of fifty trials for each data set, the CMM would take a measurement on designated workpiece components, collecting all geometrical properties that would be used later in the calculation. The numbers of measurement points used to measure the primary, secondary and tertiary planes were forty-five, twenty-four, and fifteen, respectively. Twenty-five points were used to determine the geometry of the hole. The orientation of the workpiece was obtained directly from the CMM software. The position was calculated from the direction-cosine normal to the primary plane, N_p, the hole axis, N_c, the location of the plane, P_p, and the virtual location of the feature, P_c (Figure 7). P_c could not be considered the true location of the cylindrical because the points picked on the hole's inner surface by the CMM did not guarantee complete surface coverage. The true position of the feature, O, which was theoretically at halfway on the hole axis, were located by the procedure described in the following section. To evaluate the effect of the workpiece displacement on the variability of the feature, the micrometers were used to simulate errors at the fixturing points that caused the workpiece to divert from its nominal position. The workpiece would be pulled towards the locators or the micrometers when the errors were

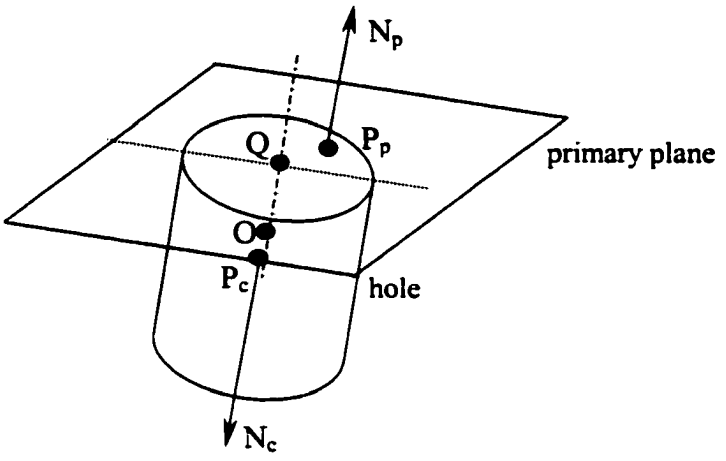

Figure 7. The determination of the workpiece or feature position.

negative and would be pushed away from the locators, otherwise. The micrometers were then repeatedly adjusted to generate the information that would be used in subsequent calculation of workpiece's position and orientation.

GEOMETRICAL ANALYSIS

Generally, the characteristic of a plane can be obtained from the following equation

$$D = P \bullet N_p \tag{16}$$

where P is a point on the plane, N_p is a normal vector to the plane, and D is a distance from the plane to the origin of the world coordinate system. In order to locate the position of the feature, the intersection point between the hole axis and the plane must be calculated. Once the point is found, it will be projected downward along the hole axis by the distance of 1 in, and there lies the position of the feature as shown in Eq (17).

$$O = Q + N_c \tag{17}$$

where

$$Q = P_c + tN_c \tag{18}$$

and

$$t = \frac{-(P_c \bullet N_p)}{N_c \bullet N_p} + D \tag{19}$$

STATISTICAL ANALYSIS

After the experiment was completed, a method of evaluating the model proficiency was carried out. The following statistical method was used to compare the experimental and theoretical data. The hypotheses were tested whether the theoretical data were valid to represent the experimental ones,

$$n(\bar{x} - \mu)' S^{-1} (\bar{x} - \mu) \leq \frac{p(n-1)}{(n-p)} F_{p,n-p}(\alpha) \tag{20}$$

where n is a sample size of the data, $\bar{x}$ is a mean of the experimental data, μ is a mean of the theoretical data, S^{-1} is a variance-covariance matrix of the experimental data, and p is a number of parameters.

If Eq. (20) is satisfied, it means that at the α level of significance the theoretical data, μ, is a plausible value for the mean of the experimental distribution. In order to test the above hypothesis, the F statistic obtained from the right term of Eq.(20) will be compared with the critical value from the other side of the inequality.

Table 6. *F* statistics for the workpiece primary plane orientation obtained from each data set compared to the critical values.

Data Set	Sample Size	Theoretical Mean	Experimental Mean	Critical Value	*F*
1	50	[-0.0021 -0.0012 0.9999]	[-0.0008 -0.0006 0.9999]	8.7320	0.9666
2	50	[0.0052 0.0005 0.9998]	[0.0057 0.0009 0.9998]	8.7320	0.1573
3	50	[-0.0010 0.0006 0.9998]	[-0.0005 0.0010 0.9998]	8.7320	0.1250
4	50	[-0.0024 0.0011 0.9994]	[-0.0018 0.0014 0.9994]	8.7320	0.0531

Table 7. *F* statistics for the workpiece secondary plane orientation obtained from each data set compared to the critical values.

Data Set	Sample Size	Theoretical Mean	Experimental Mean	Critical Value	*F*
1	50	[0.9999 -0.0011 0.0021]	[0.9999 -0.0016 0.0007]	8.7320	1.5313
2	50	[0.9998 -0.0007 -0.0052]	[0.9998 -0.0001 -0.0053]	8.7320	1.8321
3	50	[0.9998 -0.0019 0.0010]	[0.9998 -0.0016 -0.0008]	8.7320	0.5457
4	50	[0.9995 -0.0010 0.0024]	[0.9995 -0.0004 0.0026]	8.7320	2.0834

Table 8. *F* statistics for feature location obtained from each data set compared to the critical values.

Data Set	Sample Size	Theoretical Mean	Experimental Mean	Critical Value	*F*
1	50	[-2.9623 -4.0119 -1.0006]	[-2.9642 -4.0116 -1.0113]	8.7320	0.6278
2	50	[-2.9982 -3.9966 -1.0012]	[-2.9962 -3.9974 -0.9634]	8.7320	4.2673
3	50	[-3.0044 -3.9972 -1.0012]	[-3.0033 -3.9936 -0.9994]	8.7320	3.8025
4	50	[-3.0079 -3.9962 -0.9963]	[-3.0042 -3.9888 -1.0109]	8.7320	4.7906

The data collected from the experiment then were used to establish geometric variability of the cylindrical feature. Geometric variability is a diameter of a cylinder within which the actual feature is allowed to move when it is subject to errors found in manufacturing. The geometric variability is analogous to a positional tolerance zone for a hole as defined for geometric dimensioning and tolerancing. As shown in Table 6-8, all the F statistics in the last column data are less than the critical values, indicating that the means of the experimental data are reasonably represented by the theoretical ones obtained from the model developed in this work. The results in Table 9 also strongly confirm the validity of the model as the difference between the predicted and measured values were 0.09% for location and 0.009% for orientation.

Table 9. Radii of the geometric variation regions (in). Rd_1, Rd_2 and Rd_3 are the radiuses obtained from Eq. (10-12). *Top*, *mid* and *bottom* are the top, middle and bottom ellipses, which are the projections along the hole axis.

Data Set		experimental			theoretical		
		Rd_1	Rd_2	Rd_3	Rd_1	Rd_2	Rd_3
1	top	0.0011	0.0012	0.0011	0.0010	0.0010	0.0010
	mid	0.0010	0.0010	0.0010			
	bottom	0.0010	0.0010	0.0010			
2	top	0.0021	0.0022	0.0022	0.0019	0.0019	0.0019
	mid	0.0019	0.0019	0.0019			
	bottom	0.0018	0.0019	0.0018			
3	top	0.0008	0.0011	0.0010	0.0007	0.0008	0.0007
	mid	0.0007	0.0007	0.0007			
	bottom	0.0006	0.0007	0.0007			
4	top	0.0032	0.0037	0.0035	0.0027	0.0029	0.0028
	mid	0.0026	0.0028	0.0027			
	bottom	0.0024	0.0025	0.0026			

CONCLUSION

This study proposes the idea of how to integrate the variability in workpiece location and orientation to feature tolerancing. The positional tolerance of a cylindrical feature is a diameter of a cylinder in which the feature's axis must lie. To impose such tolerance efficiently, we must take into account the variability in both location and orientation of the workpiece. Such information is then combined through an appropriate geometric analysis, yielding distributions of feature position and orientation. Elliptical contours are used to represent geometric variation of the feature. Once the distribution of the axis's end points is known, a circular region as a function of workpiece displacement is established to define the positional tolerance of the feature in relation with the desired probability of acceptance, p.

Calculating the radius, of which the circular variation region containing the accurate desired probability of acceptance, is not easy. Most researchers proposed numerical methods

to estimate the true radius of the circle. The closeness to the true radius is expected to change over the desired probability and the ratio of the variances in both directions. Each formula also generates different level of accuracy. To decide which formula is best is subjective. In tolerance analysis the choice of the desired probability is selective depending upon the application and the variable nature of the feature. As a result of high probability when used with the feature with a wide variety in dimension or geometry of interest, the tolerance will tend to be too large which may lead to difficulties in assembly or subsequent applications. Manufacturers will need to reduce the variability of the feature in order to satisfy tighter tolerance. However, tighter tolerance usually is associated with high cost. The loss of area efficiency is also another issue to be aware of. Extra care must be placed on the case where the correlation among the variables is too high. Establishment of a positional tolerance of machined features involves several parameters. Each parameter has its own role controlling the mechanics of tolerancing. A designer is responsible to find the way that would benefit the production the most. As the model was proven to be efficient in evaluating the variability of workpiece components given errors at locating areas, implementing the concept proposed in this work would help the designer impose the tolerance efficiently, and consequently reduce manufacturing cost and improve product quality.

REFERENCES

1.Mansoor, E.M., *The application of probability to tolerance used in engineering designs*. Proceedings of the Institution of Mechanical Engineers, 1964. **178 Pt1**(1).

2.Nassef, A.O. and H.A. ElMaraghy, *Statistical analysis and optimal allocation of geometric tolerances.* Proceedings of the 1995 Database Symposium, ASME Database Symposium, 1995: p. 817-824.

3.Nassef, A.O. and H.A. ElMaraghy, *Allocation of geometric tolerances: New criterion and methodology.* CIRP Annals - Manufacturing Technology, 1997. **46**(1): p. 101-106.

4.Nassef, A.O. and H.A. ElMaraghy, *Determination of best objective function for evaluating geometric deviations.* International Journal of Advanced Manufacturing Technology, 1999. **15**(2): p. 90-95.

5.Nigam, S.D. and J.U. Turner, *Review of statistical approaches to tolerance analysis.* Computer Aided Design, 1995. **27**(1): p. 6-15.

6.Evans, D.H., *An application of numerical integration techniques to statistical tolerancing.* Technometrics, 1967. **9**(3): p. 441-456.

7.Evans, D.H., *An application of numerical integration techniques to statistical tolerancing, III General distributions.* Technometrics, 1972. **14**(1): p. 23-35.

8.Lin, S.-S., H.-P. Wang, and C. Zhang, *Statistical tolerance analysis based on beta distributions.* Journal of Manufacturing Systems, 1997. **16**: p. 150-8.

9.He, J.R., *Estimating the distributions of manufactured dimensions with the beta probability density function.* International Journal of Machine Tools & Manufacture, 1991. **31**(3): p. 38.-396.

10.Treacy, P., et al., *Automated tolerance analysis for mechanical assemblies modeled with geometric features and relational data structure.* Computer Aided Design, 1991. **23**(6): p. 444-453.

11.Johnson, R.A. and D.W. Wichern, *Applied Multivariate Statistical Analysis*. 4 ed. 1998, Upper Saddle River, NJ: Prentice-Hall, Inc.

12.Zeid, I., *CAD/CAM Theory and Practice*. 1991, New York, NY.: McGraw-Hill, Inc.

13.Foster, L.W., *Geo_Metrics III*. 1994, Reading, MA.: Addison-Wesley Publishing Company, Inc.

14.Chew, V., *Confidence , prediction, and tolerance regions for the multivariate normal distribution*. Journal of the American Statistical Association, 1966. **61**(315): p. 605-617.

15.Fuchs, C. and R.-S. Kenett, *Multivariate tolerance regions and F-tests*. Journal of Quality Technology, 1987. **19**: p. 122-31.

16.Gilliland, D.C., *Integral of the bivariate normal distribution over an offset circle*. Journal of the American Statistical Association, 1962. **57**: p. 758-68.

17.Hall, I.J. and D.D. Sheldon, *Improved bivariate normal tolerance regions with some applications*. Journal of Quality Technology, 1979. **11**(1): p. 13-19.

18.Harter, H.L., *Circular error probabilities*. Journal of the American Statistical Association, 1960. **55**: p. 723-31.

19.John, S., *A tolerance region for multivariate normal distributions*. Sankhya, Ser. A, 1963. **25**: p. 363-368.

20.Lowe, J.R., *A table of the integral of the bivariate normal distribution over an offset circle*. Journal of the Royal Statistical Society, Series B, 1960. **22**: p. 177-187.

21.Oberg, E.N., *Approximate formulas for the radii of circles which include a specified fraction of a normal bivariate distribution.* Annals of the Institute of Statistical Mathematics, 1947. **18**: p. 442-7.

22.Siotani, M., *Tolerance regions for a multivariate normal population.* Annals of the Institute of Statistical Mathematics, 1964. **16**: p. 135-153.

23.Weingarten, H. and A.R. DiDonato, *A table of generalized circular error.* Mathematics of Computation, 1961. **15**: p. 169-173.

CHAPTER 4. GENERAL CONCLUSION

This study consisted of two sections. First, the development of a model to determine the displacement of a workpiece subject to variable surface errors at contact locations. The model in the first section applied a step-wise movement to a prismatic workpiece, to simulate the behavior of the workpiece when brought into contact with a 3-2-1 fixture. The surface error variation at the contact points was assumed to follow a normal distribution pattern. Statistical analysis was carried out by employing two different methods, Taylor series approximations and Monte Carlo simulations, as they reduce the difficulties in computing moments of the resultant distribution. The results indicated that the discrepancies between the moments estimated from either approach were not significant. However, they both provided accurate solutions under different limitations. Taylor series is recommended whenever the variation of the variables is not large and the calculation of the partial derivatives is not too complex. Also, the assumption of independency among variables must hold. Alternatively, Monte Carlo simulation is much simpler but it requires large sample size to assure accurate results, and it may involve relatively high computational efforts.

The second part of this work was geometric variability analysis of machined features produced on a displaced workpiece. Once the model of the workpiece displacement was established, it is of interest to implement this technique to improve the quality of the features subsequently machined on that workpiece. In this second part, the effect of the workpiece displacement on the variability of feature location and orientation was investigated. Taking such effect into account, a new approach of feature tolerancing was proposed. A cylindrical feature was used as an object of study. The results suggested that the lower limit of feature

tolerance could be established when the variability of the surface errors at the contact locations and a probability of acceptance were known. In tolerance analysis, the choice of the desired probability is subject to the application and the variable nature of the feature. As a result of the high probability when used with the feature with a wide variety in dimension or geometry of interest, the tolerance will tend to be large, which may lead to difficulties in assembly or subsequent applications. Manufacturers will need to reduce the variability of the feature to make the tolerance tighter while maintaining such high probability. However, tighter tolerance is usually related to high production cost.

Not only tolerancing, the models related to workpiece displacement are expected to have even greater contribution in the future to fixture design and process planning. The fixture could be redesigned in a way that it will be able to repeatedly position the workpiece closest to its theoretical location and orientation. Contact points could be relocated to wherever offering the most accurate workpiece positioning. In critical cases, the tool path could be modified to compensate for the error initially generated by the workpiece imperfection in dimension and geometry.

In manufacturing, there are a number of factors accountable for the quality of the end products. It is sometimes inevitable to eliminate such factors that weaken the production efficiency. Being aware of their effect would discover ways that are the most beneficial to the production process. Understanding how the workpiece interacts with the fixture under less-than-perfect situation will allow us to allocate tolerances, which is one way to reduce manufacturing cost and improve product quality.

ACKNOWLEDGEMENTS

Above all, I would like to thank my major professor, Dr. Frank E. Peters for his guidance throughout my graduate studies. Culture-related confusion is among obstacles widely confronted by international students. With his generosity and supportive advice, I was able to easily adjust myself to the new community and carry out my study to the graduation day. In addition, I feel indebted for invaluable instruction from the committee members, Dr. John Jackman, Dr. Palaniappa Molian, Dr. Timothy Van Voorhis, and Dr. Stephen Vardeman.

I also feel grateful for friendship from Thai students, especially Sumate Chaiprapat, Varaporn Sangtong, Kageeporn Wongpreedee and many more. When far away from home, they were like my family making my days more colorful and lending their shoulders through my rough times. My family, though not here, is my lifetime spiritual support. I thank them for encouraging me to realize how important education is. Finally, this dissertation would not be made possible without Iowa State University. I will cherish the time I had spent here always.

APPENDIX A. WORKPIECE TRANSFORMATION

According to the assumption that the surface errors are measured normal to the workpiece planes, only the errors in these directions are thus accounted for workpiece displacement. The relationship between the nominal contact point (P_i) and the actual contact points (P_{id}) is defined as:

$$P_{id} = P_i + d_i \bar{N}_p \text{ for i=1,2, and 3} \quad \text{(A.1)}$$

$$P_{id} = P_i + d_i \bar{N}_s \text{ for i=4 and 5} \quad \text{(A.2)}$$

$$P_{id} = P_i + d_i \bar{N}_t \text{ for i =6} \quad \text{(A.3)}$$

Note that in this paper, the workpiece is virtually brought into contact with the fixture by using a step-wise process, simplified from that developed by Salisbury and Peters [1]. The initial orientation of the workpiece will have the primary, secondary and tertiary planes aligned with the z, $-x$ and y axes, respectively. This is shown in Figure A.1.

The movements to be described in the following sections are not physical but simulated. The result of these simulated moves is the same as actually occurs. The orientation of the workpiece is represented by two vectors: the normal vectors of the workpiece's primary and secondary planes, $\bar{N}_p$, $\bar{N}_s$. The target point, which signifies the workpiece location, could be any crucial point in which we desire to know the variability of its location after fixturing. The target point could be the reference point of a feature to be produced. Throughout this paper, any reference to the primary, secondary and tertiary planes will be referred to as those of the workpiece, unless otherwise stated.

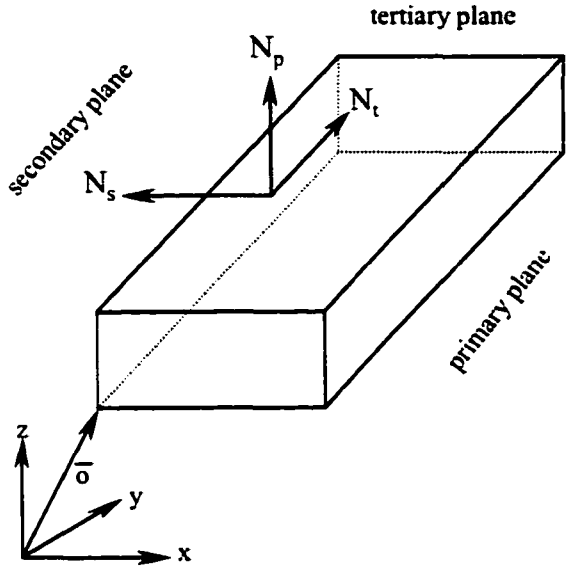

Figure A.1. The initial position and orientation of a workpiece before applying virtual movement.

PRIMARY PLANE

The displacement of the workpiece as a result of the errors at the primary plane locators is determined via a translation and rotation of the workpiece.

TRANSLATION

The nominal position of the target point is located by $\bar{o}$ with respect to the fixture reference system. The algorithm begins with translating the workpiece up or down along z axis until the workpiece makes contact with any one of the three primary plane locators, named P_{1d}. The position of the workpiece is now defined by Eq. (A.4).

$$\bar{o}_{pt} = \bar{o} + d_1 \bar{N}_p \tag{A.4}$$

ROTATION

In the presence of variability in the primary plane, the orientation of the plane is slightly different from the nominal direction. Once the workpiece has made contact with all three locators in the primary plane, the normal vector of the plane is

$$\bar{N}'_p = \overrightarrow{P_{1d}P_{2d}} \times \overrightarrow{P_{1d}P_{3d}} \tag{A.5}$$

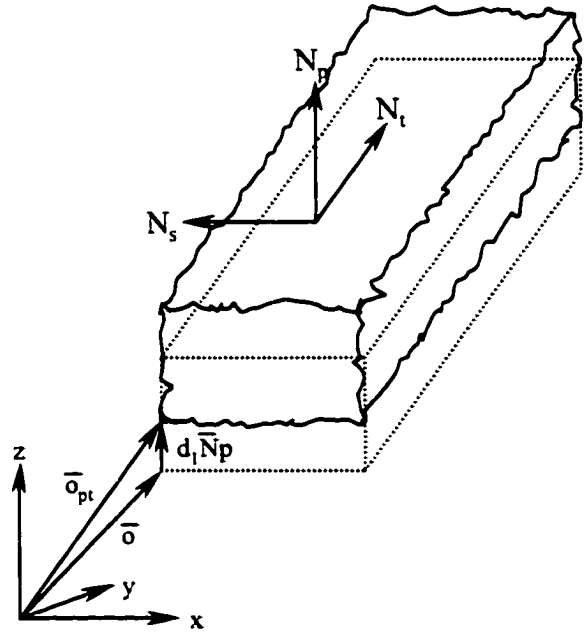

Figure A.2. Translation in the primary plane.

Since the workpiece is assumed to be a rigid body, the orientation of the other two planes can be attained by employing the following transformation matrix. The general form of a rotational transformation matrix is:

$$T(\phi,u)=\begin{bmatrix} u_x^2V(\varphi)+C(\phi) & u_xu_yV(\phi)-u_zS(\phi) & u_xu_zV(\phi)+u_yS(\phi) \\ u_xu_yV(\phi)+u_zS(\phi) & u_y^2V(\phi)+C(\phi) & u_yu_zV(\phi)-u_xS(\phi) \\ u_xu_zV(\phi)-u_yS(\phi) & u_yu_zV(\phi)+u_xS\phi & u_z^2V(\phi)+C(\phi) \end{bmatrix} \quad \text{(A.6)}$$

where ϕ = an angle, u = axis of rotation, $C(\phi) = \cos(\phi)$, $S(\phi) = \sin(\phi)$ and $V(\phi) = 1-\cos(\phi)$.

The axis of rotation can be derived from

$$u_p = \bar{N}_p \times \bar{N}'_p \quad \text{(A.7)}$$

The angle of rotation can be found with Eq. (A.8).

$$\theta_p = \cos^{-1}(\bar{N}_p \bullet \bar{N}'_p) \quad \text{(A.8)}$$

The rotational transformation matrix due to the surface errors in the primary plane is then

$$T_p = T(\theta_p, u_p) \quad \text{(A.9)}$$

The orientation of the secondary and tertiary planes are now deviated to

$$\bar{N}'_s = T_p * \bar{N}_s \quad \text{(A.10)}$$

$$\bar{N}'_t = T_p * \bar{N}_t \quad \text{(A.11)}$$

The new vector to the target point is found by Eq. (A.12). The workpiece after these transformations is shown in Figure A.3.

$$\bar{o}_{pr} = T_p * \bar{o}_{pt} \quad \text{(A.12)}$$

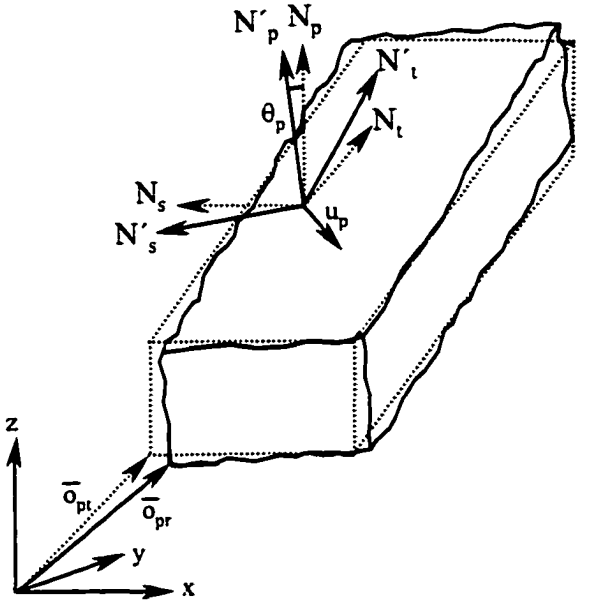

Figure A.3. The deviation of workpiece position and orientation due to the surface errors on the primary plane locators.

SECONDARY PLANE

The errors at the contact points in the secondary plane cause the deviation of the workpiece, which can be represented by the transformations developed in the following sections.

TRANSLATION

The workpiece is translated to make contact with one of the locators of the secondary plane, named P_{4d} (Figure A.4). The general equation of the distance, D, from a point $P_{x,y,z}$ to a plane which is at a distance of l from the origin is

$$D = \left| N_x P_x + N_y P_y + N_z P_z - l \right| \qquad \text{(A.13)}$$

where $N_{x,y,z}$ is a normal vector of the plane

The distance from the secondary plane of the workpiece to P_{4d} is shown in Eq. (A.14).

$$D_s = \left| N'_{sx} P_{4dx} + N'_{sy} P_{4dy} + N'_{sz} P_{4dz} - l_s \right| \qquad \text{(A.14)}$$

The unknown at this time is l_s, however it is not straightforward to determine its value. By definition, l_s is the distance from the origin to the deviated secondary plane, along the direction normal to the plane. Since the orientation of the deviated secondary plane is already given in Eq. (A.10), the calculation for l_s only requires a point on the plane denoting the current location of the plane to use in Eq. (A.16). This point can be obtained by applying the transformations caused by the surface errors in the primary plane to any point lying on the initial secondary plane. If we look back to the beginning when the workpiece was at its nominal location and orientation, the nominal plane was in touch with the locators P_4 and P_5. Since P_4 and P_5 were actually lying on the initial secondary plane, either one of them can be used to calculate the current location of the plane. We will select P_4. As the workpiece moves according to the transformations in consequence of the surface errors in the primary plane, P_4 travels as well in accordance to Eq. (A.15). By substituting P_{4t} into Eq. (A.16), we are now able to locate the secondary plane relative to the origin of the fixture reference system.

$$P_{4t} = T_p * (P_4 + d_1) \qquad \text{(A.15)}$$

where P_{4t} is the new location of P_4 after application of the transformation of the primary plane.

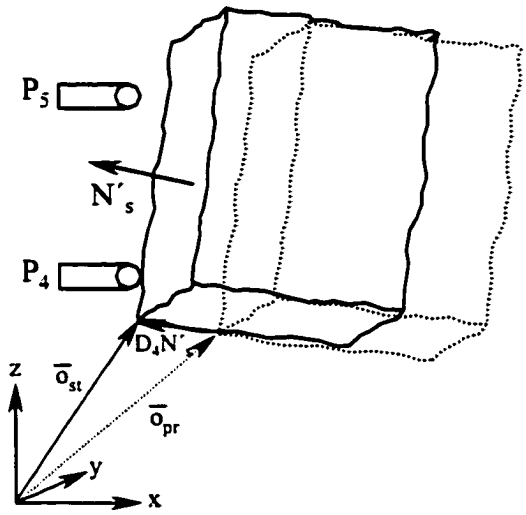

Figure A.4. Translation of the workpiece to make contact with the first locator on the secondary plane.

The normal distance between the plan on which P_{4t} lies and the origin is

$$l_s = N_s' \bullet P_{4t} \tag{A.16}$$

By substituting l_s into Eq. (A.14), we will be able to derive D_s, distance between the locator P_{4d} and the secondary plane. In other words, it is the distance that the workpiece will be translated to make contact with P_{4d} and the current location of the target point on the workpiece is

$$\bar{o}_{st} = \bar{o}_{pr} + D_s \bar{N}_s' \tag{A.17}$$

ROTATION

The workpiece has translated to make contact with P_{4d}, and it now will be rotated about P_{4d} to touch P_{5d} completing the contact with the secondary plane. The normal vector of the secondary plane after rotation about P_{4d} to P_{5d} is:

$$\bar{N}_s'' = \bar{N}_p' \times \overrightarrow{P_{4d}P_{5d}} \tag{A.18}$$

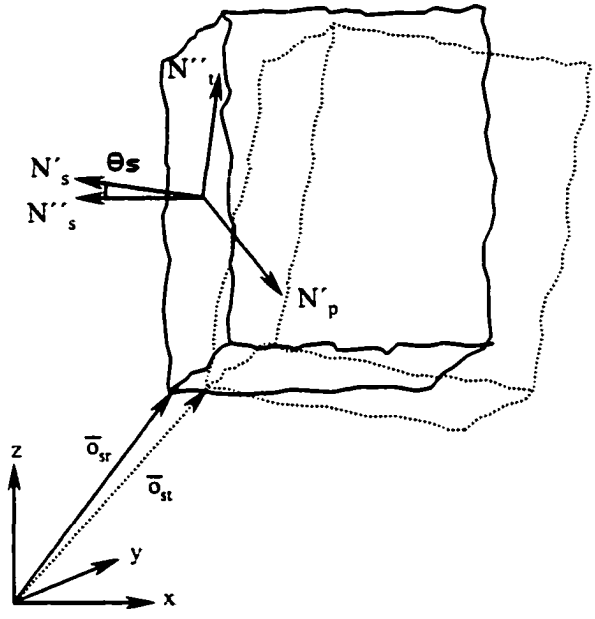

Figure A.5. Rotation about the first contact point of the secondary plane in order to make contact with the second point.

The axis of rotation can be derived from

$$u_s = \bar{N}_s' \times \bar{N}'' \tag{A.19}$$

The angle of rotation is found as follows:

$$\theta_s = \cos^{-1}(\bar{N}_s' \bullet \bar{N}_s'') \tag{A.20}$$

The normal vectors of the secondary and tertiary planes can be determined by Eq. (A.21) and (A.22). The transformation matrix, T_s, is found by substituting $\phi = \theta_s$ and $u = u_s$ into Eq. (A.6). During this transformation, the orientation of the primary plane will remain unchanged since the rotation is made around its current normal vector.

$$\bar{N}_s'' = T_s * \bar{N}_s' \tag{A.21}$$

$$\bar{N}_t'' = T_s * \bar{N}_t' \tag{A.22}$$

The target point is now located at

$$\bar{o}_{sr} = T_s * \bar{o}_{st} \tag{A.23}$$

TERTIARY PLANE

For the final transformation, the workpiece will again be translated: this time it is moved toward the tertiary plane to make contact with P_{6d} as shown in Figure A.6. The translation distance is obtained from Eq. (A.24).

$$D_t = \left| N_{tx}'' P_{6dx} + N_{ty}'' P_{6dy} + N_{tz}'' P_{6dz} - l_t \right| \tag{A.24}$$

To obtain l_t, we will follow the steps of the derivation of l_s in the previous section except we use P_6 instead of P_4 and the transformation is different as shown in Eq. (A.25).

$$P_{6t} = T_s * ((T_p * (P_6 + d_1)) + D_s) \tag{A.25}$$

$$l_t = N_t'' \bullet P_{6t} \tag{A.26}$$

The location of the workpiece is now

$$\bar{o}_t = \bar{o}_{sr} + D_t \bar{N}_t'' \tag{A.27}$$

The final location and orientation of the workpiece is defined by Eq. (A.5), (A.18) and (A.27).

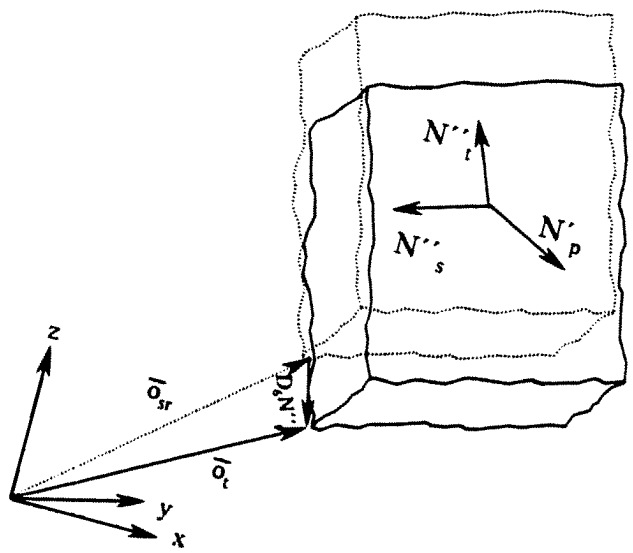

Figure A.6. Translation in the tertiary plane.

APPENDIX B

DISTRIBUTION OF FEATURE POSITION

It is assumed that the workpiece position (and hole position), is multivariate normally distributed with

$$\mu_P = [\mu_{P1}, \mu_{P2}, \mu_{P3}] \tag{B.1}$$

$$\Sigma_P = \begin{bmatrix} \sigma_{P1}^2 & \sigma_{P12} & \sigma_{P13} \\ \sigma_{p21} & \sigma_{p2}^2 & \sigma_{P23} \\ \sigma_{P31} & \sigma_{P32} & \sigma_{P3}^2 \end{bmatrix} \tag{B.2}$$

The contour of a constant density for a multivariate normal distribution with $n = 3$ is pictured like an ellipsoid defined by Eq. (B.3).

$$(x-\mu)'\Sigma^{-1}(x-\mu) \le c^2 \tag{B.3}$$

where c^2 depends upon the desired volume of the ellipsoid.

For 95% probability of a bivariate normal distribution, c^2 will equal 5.99. The elliptical contour is theoretically centered at the mean of the distribution, μ, and its axes are governed by the eigenvalues, λ, and eigenvectors, e, of the covariance matrix, Σ, (Figure B.1). The eigenvalues and eigenvectors of Σ are defined by

$$|\Sigma - \lambda I| = 0 \tag{B.4}$$

$$\Sigma e = \lambda e \tag{B.5}$$

From Eq.(B.5), the eigenvalues of Σ_P are

$$\lambda = \frac{(\sigma_{P1}^2 + \sigma_{P2}^2) \pm \sqrt{(\sigma_{P1}^2 - \sigma_{P2}^2)^2 + 4\sigma_{P12}^2}}{2} \tag{B.6}$$

Eigenvectors that correspond to the above eigenvalues are

$$v_1 = [\frac{(\sigma_{P1}^2 - \sigma_{P2}^2) + \sqrt{(\sigma_{P2}^2 - \sigma_{P1}^2)^2 + 4\sigma_{P12}^2}}{2\sigma_{P12}}, 1] \quad \text{(B.7)}$$

$$v_2 = [\frac{(\sigma_{P1}^2 + \sigma_{P2}^2) - \sqrt{(\sigma_{P2}^2 - \sigma_{P1}^2)^2 + 4\sigma_{P12}^2}}{2\sigma_{P12}}, 1] \quad \text{(B.8)}$$

Once we have the eigenvalues and eigenvectors of the covariance matrix, we are able to draw an ellipse, which contains the desired probability and orientation for the distribution.

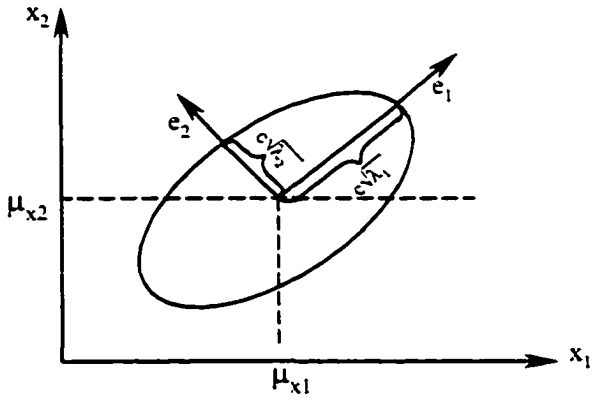

Figure B.1. The contour of a bivariate normal distribution

DISTRIBUTION OF AXIS ORIENTATION

For the ease of analyzing the distribution of axis orientation, we establish a new model similar to the existing one with the workpiece initially being at its nominal location and orientation. In the new model, instead of transforming the workpiece, an equivalent transformation is implemented to the cutter, which has the same result. Figure B.2 illustrates the normal vectors and cutting directions of the actual displaced workpiece, compared to those in the new model. In the figure, N_i are the normal vectors of the workpiece and C_i are

the cutter directions. Obviously, the axis C_2 actually is a reflection of the normal vector N_1 having N_2 or C_1 being a centerline.

N_i are related to each other by

$$N_t = T * N \tag{B.9}$$

where T is a transformation matrix.

Transforming N_1 to N_2 is based on the fact that the direction of a vector in space is not changed by translation but rotation, T is thus simply a rotation matrix. The general form of a rotation matrix is shown below.

$$T(\phi,u)=\begin{bmatrix} u_x^2V(\phi)+C(\phi) & u_xu_yV(\phi)-u_zS(\phi) & u_xu_zV(\phi)+u_yS(\phi) \\ u_xu_yV(\phi)+u_zS(\phi) & u_y^2V(\phi)+C(\phi) & u_yu_zV(\phi)-u_xS(\phi) \\ u_xu_zV(\phi)-u_yS(\phi) & u_yu_zV(\phi)+u_xS\phi & u_z^2V(\phi)+C(\phi) \end{bmatrix} \tag{B.10}$$

where ϕ = an angle, u = axis of rotation, $C(\phi) = \cos(\phi)$, $S(\phi) = \sin(\phi)$ and $V(\phi) = 1-\cos(\phi)$.

If $N_2 = [0, 0, 1]$ and N_1 is given as $[N_x, N_y, N_z]$, then by applying the transformation steps from the previous paper we obtain the following.

$$u = \vec{N}_1 \times \vec{N}_2 \tag{B.11}$$

$$u = [\frac{N_y}{\sqrt{N_x^2+N_y^2}}, \frac{-N_x}{\sqrt{N_x^2+N_y^2}}, 0] \tag{B.12}$$

and the angle of rotation;

$$\phi = \cos^{-1}(\vec{N}_1 \bullet \vec{N}_2) \tag{B.13}$$

$$\phi = acos(N_z) \tag{B.14}$$

Then we substitute u and ϕ into the rotation matrix in Eq. (B.10). C_2 is derived from transforming C_1, which we assume to be [0 0 1], by T.

$$C_2 = [\frac{-N_x\sqrt{(1-N_z^2)}}{\sqrt{N_x^2+N_y^2}}, \frac{-N_y\sqrt{(1-N_z^2)}}{\sqrt{N_x^2+N_y^2}}, N_z] \quad \text{(B.15)}$$

Since N_1 is a unit vector, $N_x^2 + N_y^2 + N_z^2 = 1$ then

$$C_1 = [-N_x, -N_y, N_z] \quad \text{(B.16)}$$

Clearly, the mean of C_2 is actually the reflection of the mean of N_1 and it also can be proved that the variance of C_2 and N_1 are the same.

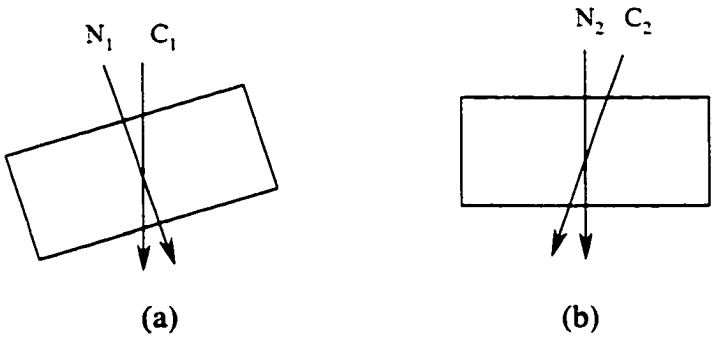

Figure B.2. (a) cutting direction when the workpiece is displaced. (b) when the workpiece is transformed back to nominal orientation

We now have the distribution of both the feature position and the axis orientation as functions of given distributions of the workpiece location and orientation. This information will be combined to establish the positional tolerance of the feature.

DISTRIBUTION OF PROJECTED POINTS

Be reminded that the positional tolerance zone of the cylindrical feature is a cylinder which must contain the feature's axis. We assume that the distribution of the feature position (workpiece position) is known. Because variability in the orientation of the axis exists, the

projections onto the top and bottom planes of an elliptical cloud representing the variability of the feature position along the feature axes will be different in shape from the original cloud. The cloud will vary not only due to the erratic orientation of the axes, but also their length. To find the positional tolerance, we begin by calculating the top and bottom projections. Let n_i be a unit normal vector of the plane through which the feature will be machined.

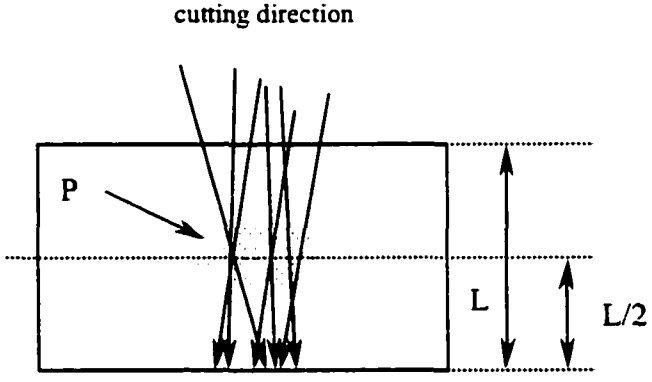

Figure B.3. The effect of orientation variability on the projections of the feature position on the top and bottom plane of the workpiece

The equation of the axis in 3-dimensional space, at given p, is

$$\frac{x-p_1}{n_1}=\frac{y-p_2}{n_2}=\frac{z-p_3}{n_3}=t \tag{B.17}$$

or

$$x=p_1+n_1t\,,\,y=p_2+n_2t\,,\,z=p_3+n_3t \tag{B.18}$$

where $[n_1, n_2, n_3]$ is the direction cosine of the line

The general equation of the plane is

$$ax+by+cz=d \tag{B.19}$$

In case that the plane is oriented parallel to X-Y plane, Eq. (B.19) will become

$$z = d \tag{B.20}$$

From Eq. (B.18) and (B.20), the line will intersect the plane at

$$t = \frac{d - p_3}{n_3} \tag{B.21}$$

Substituting Eq. (B.21) into Eq. (B.18) results in

$$x = p_1 + n_1(\frac{d - p_3}{n_3}), y = p_2 + n_2(\frac{d - p_3}{n_3}), z = d \tag{B.22}$$

where

$d = L$ when the plane on which the points are projected is the top plane, and $[n_1, n_2, n_3]$ is the direction cosine of the normal vector of the top plane.

$d = 0$ when the plane on which the points are projected is the bottom plane, and $[-n_1, -n_2, -n_3]$ is the direction cosine of the normal vector of the bottom plane.

Let's call the projections of the points representing the feature position on the top and bottom planes of the workpiece, "A."

Linearizing Eq. (B.22) around μ_i gives

$$A \sim N(\mu_A, F(\mu)\Sigma_a F'(\mu)) \tag{B.23}$$

where $A = \begin{bmatrix} X \\ Y \\ Z \end{bmatrix}$, $A(\mu) = \begin{bmatrix} \mu_{P1} + \mu_{N1}(\frac{d-\mu_{P3}}{\mu_{N3}}) \\ \mu_{P2} + \mu_{N2}(\frac{d-\mu_{P3}}{\mu_{N3}}) \\ D \end{bmatrix}$, $\Sigma_a = \begin{bmatrix} \Sigma_P & \vdots & \Sigma_{PN} \\ \cdots & \cdots & \cdots \\ \Sigma_{NP} & \vdots & \Sigma_N \end{bmatrix}$ and

$$F(\mu) = \begin{bmatrix} \frac{\partial X(\mu)}{\partial \mu_{P1}} & \cdots & \frac{\partial X(\mu)}{\partial \mu_{N3}} \\ \frac{\partial Y(\mu)}{\partial \mu_{P1}} & \cdots & \frac{\partial Y(\mu)}{\partial \mu_{N3}} \\ \frac{\partial Z(\mu)}{\partial \mu_{P1}} & \cdots & \frac{\partial Z(\mu)}{\partial \mu_{N3}} \end{bmatrix} = \begin{bmatrix} 1 & 0 & \frac{-\mu_{N1}}{\mu_{N3}} & (\frac{d-\mu_{P3}}{\mu_{N3}}) & 0 & -\frac{\mu_{N1}(d-\mu_{P3})}{\mu_{N3}^2} \\ 0 & 1 & \frac{-\mu_{N2}}{\mu_{N3}} & 0 & (\frac{d-\mu_{P3}}{\mu_{N3}}) & -\frac{\mu_{N2}(d-\mu_{P3})}{\mu_{N3}^2} \\ 0 & 0 & 0 & 0 & 0 & 0 \end{bmatrix} \quad \text{(B.24)}$$

Sangnui and Peters quantified the variation in location and orientation of a fixtured workpiece. This work uses this variation as input to determine the variation of a machined feature created on that fixtured workpiece. We will use Eq. (B.23) to accomplish this goal. The feature is to be machined normal to the plane, and the mean of the plane's normal vector, $\begin{bmatrix} \mu_{N1} \\ \mu_{N2} \\ \mu_{N3} \end{bmatrix}$, is $\begin{bmatrix} 0 \\ 0 \\ 1 \end{bmatrix}$. Substitute $\begin{bmatrix} \mu_{N1} \\ \mu_{N2} \\ \mu_{N3} \end{bmatrix}$ with $\begin{bmatrix} 0 \\ 0 \\ 1 \end{bmatrix}$ and μ_{P3} with $\frac{L}{2}$ into Eq. (B.24), and we obtain

$$F(\mu) = \begin{bmatrix} 1 & 0 & 0 & \frac{2d-L}{2} & 0 & 0 \\ 0 & 1 & 0 & 0 & \frac{2d-L}{2} & 0 \\ 0 & 0 & 0 & 0 & 0 & 0 \end{bmatrix} \quad \text{(B.25)}$$

Results from Chapter 2 also indicated the insignificant role of Σ_{NP} and Σ_N compared to Σ_P, leading to

$$\Sigma_a \approx \begin{bmatrix} \Sigma_P & \vdots & 0 \\ \cdots & \cdots & \cdots \\ 0 & \vdots & 0 \end{bmatrix} \tag{B.26}$$

From Eq. (B.23), we know that $\Sigma_A = F(\mu)\Sigma_a F'(\mu)$.

$$\Sigma_A = \begin{bmatrix} \sigma_{P1}^2 & \sigma_{P12} & 0 \\ \sigma_{P12} & \sigma_{P2}^2 & 0 \\ 0 & 0 & 0 \end{bmatrix} \tag{B.27}$$

The information we have so far points out to the following conclusions.

1. Regarding Eq. (B.27), the third component of the feature position is dropped down leaving the distribution of A as the projection of the feature position distribution on the X-Y plane.

2. The previous chapter indicates negligible variability in the workpiece orientation resulting in the projections on both top and bottom plane being the same. However, when the workpiece thickness, L, becomes very large (a rare event), this conclusion may not be valid. Therefore, we can assume both projections share the same properties only when the axis orientation variability has a slight role and L is not extremely great in size.

3. Based on the assumption that the feature position is distributed as multivariate normal and on the property of such distributions that all subsets of the components have a (multivariate) normal distribution, A is also (multivariate) normally distributed with an elliptical distribution contour.